Analysis of Wavelength Shift Keying Technique with Dispersion Management Scheme to Reduce Four-Wave Mixing Effect in Optical WDM System

by

Mohammad Faisal

A thesis submitted to the Department of Electrical and Electronic Engineering of Bangladesh University of Engineering and Technology in partial fulfillment of the requirement for the degree of

MASTER OF SCIENCE IN ELECTRICAL AND ELECTRONIC ENGINEERING

Department of Electrical and Electronic Engineering

BANGLADESH UNIVERSITY OF ENGINEERING AND TECHNOLOGY

2003

APPROVAL CERTIFICATE

The thesis titled ***"Analysis of Wavelength Shift Keying Technique with Dispersion Management Scheme to Reduce Four-Wave Mixing Effect in Optical WDM System"*** Submitted by Mohammad Faisal, Roll No.: 100106260P, Session: October 2001 has been accepted as satisfactory in partial fulfillment of the requirement for the degree of Master of Science in Electrical and Electronic Engineering on December 25, 2003.

BOARD OF EXAMINERS

1. 25.12.03 — Chairman

Dr. M. Nazrul Islam
Associate Professor
Department of Electrical and Electronic Engineering
BUET, Dhaka-1000, Bangladesh

2. 25/12/03 — Member

Dr. Satya Prasad Majumder
Professor
Department of Electrical and Electronic Engineering
BUET, Dhaka-1000, Bangladesh

3. 25/12/03 — Member

Dr. Md. Saifur Rahman
Professor
Department of Electrical and Electronic Engineering
BUET, Dhaka-1000, Bangladesh

4. 25/12/03 — Member (Ex-Officio)

Dr. Mohammad Ali Choudhury
Professor & Head
Department of Electrical and Electronic Engineering
BUET, Dhaka-1000, Bangladesh

5. — Member (External)

Dr. Farruk Ahmed 25.12.03
Professor
Department of Applied Physics and Electronics
Dhaka University, Dhaka-1000, Bangladesh

DECLARATION

It is hereby declared that this thesis or any part of it has not been submitted elsewhere for the award of any degree or diploma.

Signature of the candidate

(Mohammad Faisal)

DEDICATED TO MY PARENTS

CONTENTS

Chapter 6: FWM Reduction by a Combination of WSK-WDM and Dispersion Management

Chapter 7: Conclusion

List of Figures

List of Tables

List of Symbols

α	attenuation constant
β	propagation constant
$\Delta\beta$	propagation constant difference
$\boldsymbol{k}$	wave vector
n	fiber refractive index
χ	fiber nonlinear susceptibility
η	efficiency of FWM generation
κ	fiber nonlinearity
$\chi^{(3)}$	third-order nonlinear susceptibility
ϕ	propagation phase
$\Delta\phi$	propagation phase difference
L	fiber length
L_{eff}	effective length of fiber
L_{coh}	coherence length of fiber
D_c	fiber chromatic dispersion
A_{eff}	effective core area of fiber
c	speed of light
λ	wavelength
N	number of channels
R	photodetector's responsivity
η_q	quantum efficiency of photodetector
N_{th}	thermal noise
N_{sh}	shot noise
Q	complementary error function or co-error function

P_e	probability of error or bit-error rate
f_0	zero-dispersion frequency
L_r	insertion loss
x	signal-to-noise ratio
σ	variance
B_e	electrical bandwidth of the receiver
P_{ijk}	FWM power
C_{im}^{m}	effective FWM crosstalk
P_p	power penalty
$\boldsymbol{P}_{NL}$	nonlinear polarization
ε_0	permittivity of vacuum

List of Abbreviations

SNR	Signal-to-Noise Ratio
BER	Bit Error Rate
WSK	Wavelength Shift Keying
WDM	Wavelength Division Multiplexing
DWDM	Dense Wavelength Division Multiplexing
FDM	Frequency Division Multiplexing
SRS	Stimulated Raman Scattering
SBS	Stimulated Brillouin Scattering
FWM	Four-Wave Mixing
SPM	Self Phase Modulation
XPM	Cross Phase Modulation
US	Unequal channel Spacing
RUS	Repeated Unequal channel Spacing
EDFA	Erbium-Doped Fiber Amplifier
LED	Light Emitting Diode
LASER	Light Amplification by Stimulated Emission of Radiation
APD	Avalanche Photodiode
ISI	Inter Symbol Interference
SMF	Single Mode Fiber
DSF	Dispersion Shifted Fiber
NDSF	Non Dispersion Shifted Fiber
NZDSF	Non-Zero Dispersion Shifted Fiber
DCF	Dispersion Compensating Fiber
OOK	On-Off Keying
MUX	Multiplexer
DeMUX	Demultiplexer

Acknowledgements

I am highly pleased to express my sincere and profound gratitude to my supervisor Dr. M. Nazrul Islam, Associate Professor, Department of Electrical and Electronic Engineering (EEE), Bangladesh University of Engineering and Technology, Dhaka, for providing me the opportunity to conduct graduate research in optical communications. I wish my hearty thanks to him for his continuous guidance, suggestions and wholehearted help throughout the course of the work.

I would like to express my special thanks to Dr. Satya Prasad Majumder, Professor, Department of EEE, BUET, for his invaluable suggestions and discussions.

I am grateful to Dr. James F. Young, Professor of Electrical and Computer Engineering, Rice University, USA, for providing the materials related to my research work and for his generous support.

I would also like to thank my colleagues, specially, Md. Ziaur Rahman Khan, Shaikh Anowarul Fattah, Mrs. Celia Shahnaz, Ataur Rahman Sarker, Muhammad Zulfiker Alam, Abul Bashar Mohammad Isteak Hossain and Md. Forkan Uddin for their support and continuous encouragement. I am also thankful to all personnel of departmental library, BUET reference library, Xerox section and IEEE Bangladesh section.

I like to express my heartfelt thanks and the deepest gratitude to my wife Naima Kabir, my beloved daughter and other family members for their invaluable encouragement and patience.

Finally, I am grateful to Almighty Allah for enabling me to complete the thesis.

Abstract

Optical wavelength division multiplexing (WDM) system using low dispersion fibers and erbium-doped fiber amplifiers (EDFA) is getting tremendous popularity for communication networks due to its high information capacity, high-channel-count and low system costs. WDM transmission systems effectively exploit the huge potential bandwidth of an optical fiber. More than thousand channels can be multiplexed with high bit rate if the fiber low dispersion region around 1.55 μm is fully utilized where attenuation loss is minimum and EDFA provides gain. However, a number of nonlinear effects arise due to low dispersion and high transmitting power, which severely degrade the system performance. Among these nonlinear processes, four-wave mixing (FWM) is the most serious effect that limits the allowable input power and system capacity by generating new waves, which cause performance degradation of long-haul multi-channel lightwave transmission systems.

In this thesis the performance of wavelength shift keying (WSK) technique in reducing the effect of FWM in an optical WDM system is analyzed. WSK-WDM system is a modification of the conventional WDM system that uses symmetric wavelength assignment and balanced detection to mitigate the FWM crosstalk. Performance criteria like probability of error, power penalty, allowable input power and bit rate-distance product are estimated. The performance is evaluated for different types of fibers, different number of channels, different channel spacings and different length of fibers. It is observed that the conventional on-off WDM system suffers severe performance degradation due to FWM interference particularly when fiber length, number of channels or transmitting power is high. WSK-WDM is a simple scheme to reduce this effect and excels conventional WDM at all signal power levels and allows higher allowable input power and larger bit rate-distance product for a given bit error rate. The performance of WSK-WDM is compared to that of conventional on-off WDM system and also to unequal channel spacing and repeated unequal channel spacing schemes. New schemes are proposed, which are the combinations of WSK technique and different dispersion

management techniques. The combined systems offer much enhanced performance like lower error probability, much lower power penalty and higher allowable input power per channel and greater bit rate-distance product to achieve a given bit error rate compared to those of WSK-WDM. The results obtained from this work will be useful for designing very high capacity long-haul optical communication systems.

Chapter 1

INTRODUCTION

1.1 Communication System

Communication is the process of transferring information or message like voice, video, text, data, picture, etc. from one distant place to another. Communication system is a technique/method by which two or more entities exchange their information. The basic principle of a communication system is shown in Figure 1.1, the function of which is to convey the signal from the information source over the transmission medium to the destination.

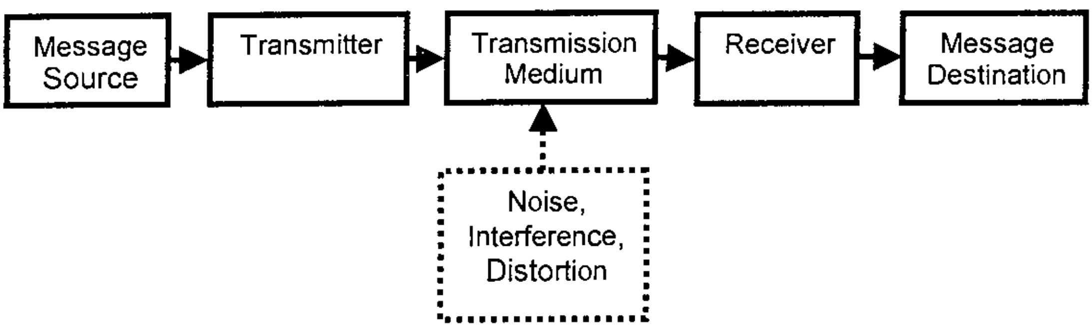

Figure 1.1: Block diagram of a general communication system

Any communication system is composed of the following basic components:

(1) Transmitter: Manipulates the information from the message source and couples it into a transmission channel in the form of a signal, which matches the transfer properties of the channel.

(2) Channel: Bridges the distance between the transmitter and receiver. As signal propagates through the channel, it gets attenuated due to transmission loss and distorted due to various nonlinear effects and interference.

(3) Receiver: Extracts the weakened and distorted signal from the channel, demodulates it, amplifies it and restores it to its original form and then passes it into the message destination.

The preliminary communication systems utilized physical methods to convey message. Use of signal fires, reflecting mirrors, signaling lamps were common forms of communication. Also birds and people were employed to carry the message. With the development of science, electrical methods of communication system have been devised. Communication was build up by varying the current amplitude and passing the current through a conductor. Then came the wireless communication. Electromagnetic waves can carry large amount of information without the need of any physical medium. Electromagnetic waves proved suitable carriers for information transfer in the atmosphere, being far less affected by the atmospheric conditions. However, their use is limited in the amount of information they can convey by their frequencies, because the information carrying capacity is directly related to the bandwidth or frequency extent of the modulated carrier. For this reason, radio communication was developed to higher frequencies (i.e., VHF, UHF etc.) leading to the introduction of the even higher frequency microwave and, latterly, millimeter wave transmission.

1.2 Evolution of Optical Communication

The increasing demand of utilizing higher frequencies led to the development of optical communication as shown in Figure 1.2. Because the optical frequencies are of the order of 10^{14} Hz, so optical communication has a theoretical information capacity exceeding that of microwave communication by a factor of 10^5.

There is, of course, nothing new in the use of optical frequencies for transmission of information. Visual methods of communication are widely used in the animal kingdom. Man has used smoke signals or reflected sunlight during day and fire beacons at night. More recently, signaling lamps have provided successful information transfer. As early as 1880, Alexander Graham Bell reported the transmission of speech using a light beam. The photophone proposed by Bell, just four years after the invention of the telephone, modulated the sunlight with a diaphragm giving speech transmission over a distance of 200 m. However, the use of optical communication was limited to short distance, low capacity communication links. This was due to both the lack of suitable light sources and the problem that light transmission in the atmosphere is restricted to the line of sight and hence severely affected by disturbances such as rain, snow, fog, dust and atmospheric turbulence. The transmitted signal was subjected to being scattered or blocked entirely by physical obstacles, and unfortunately, for those whose messages were confidential, anyone could intercept the signal. Therefore a better lightwave communication system would certainly need a light guided to help preserve the signal and so increase the reliability and distances of transmission.

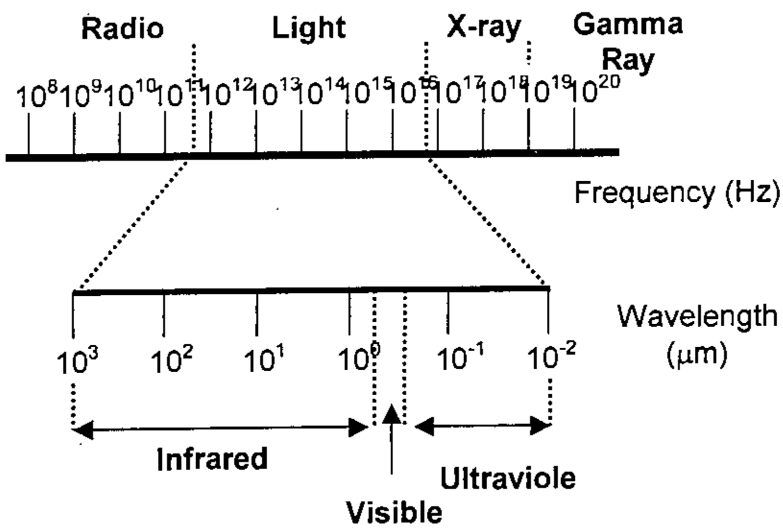

Figure 1.2: Spectrum of electromagnetic waves.

Attempts to guide the light appear to have been as early as in 1854 by producing reflections in a curved stream of water coming out of a hole in the side of a pail. Then in 1910 a solid cylinder was envisaged to guide a wide range of electromagnetic waves including the upper limits of visible light. Another light guide was developed consisting of a hollow tube with a highly reflective metal coating on its inner surface. However, the devices had high signal loss.

Essentially fiber optic communication system arose from a merging of two unrelated technologies: semiconductor technology for light sources and detectors, and optical waveguide technology for the transmission medium. The development of LASER in 1960 was a landmark for optical communication. Glass and solid state lasers were developed for use as coherent light source. Also light emitting diodes (LED), p-i-n and avalanche photodetectors have made optical communication useful and efficient. And the advent of optical amplifiers like erbium-doped fiber amplifiers (EDFA) and praseodymium-doped fluoride fiber amplifier (PDFFA) have created a revolutionary change in optical communication [1]. Optoelectronic amplifiers are now replaced by fiber amplifiers.

Experiments on glass fibers were carried out in 1930s for use as light guide. Optical fibers were used for other purposes also, such as light conduits for card readers, in material endoscopes, in photography etc. The major breakthrough in the development of optical fiber came with its use in telecommunications in the mid sixties. Researchers from UK, West Germany and France proved that exceptionally pure optical fiber was theoretically capable of guiding a light signal with very small losses. Nippon Glass Company of Japan first developed graded index fibers in 1968. Corning Glass Works of US produced fibers in 1970 with sufficient purity for use in telecommunication industry, having a loss of less than 20 dB/km [2].

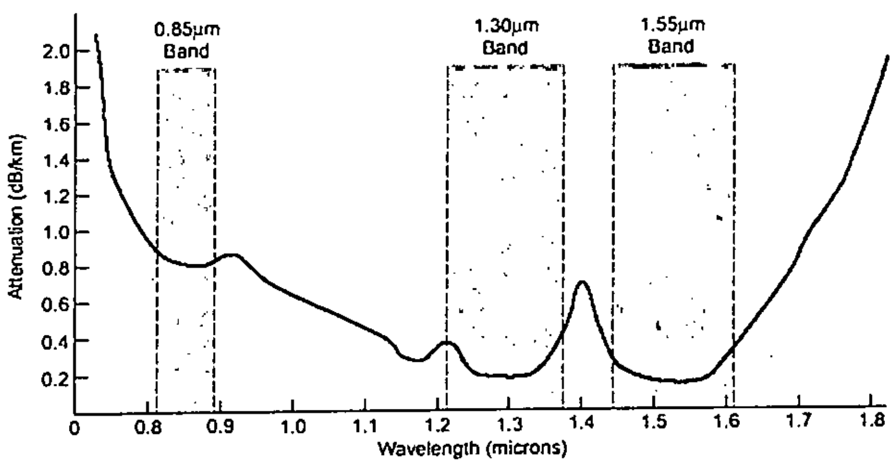

Figure 1.3: Variation of attenuation with wavelength [2]

Rapid progress has been made in both lowering the attenuation loss in fiber and increasing the wavelength it can handle. Early interest in the fiber was in the 800-900 nm wavelength region where fibers exhibited a local attenuation minimum. Later interests extended over a wider range of wavelengths up to 1300 nm and recently to 1550 nm, which offers much lower attenuation (~0.2dB/km) [3].

with an optical fiber communication system is more efficient, requiring lower signal to noise ratio at the receiver than analog modulation.

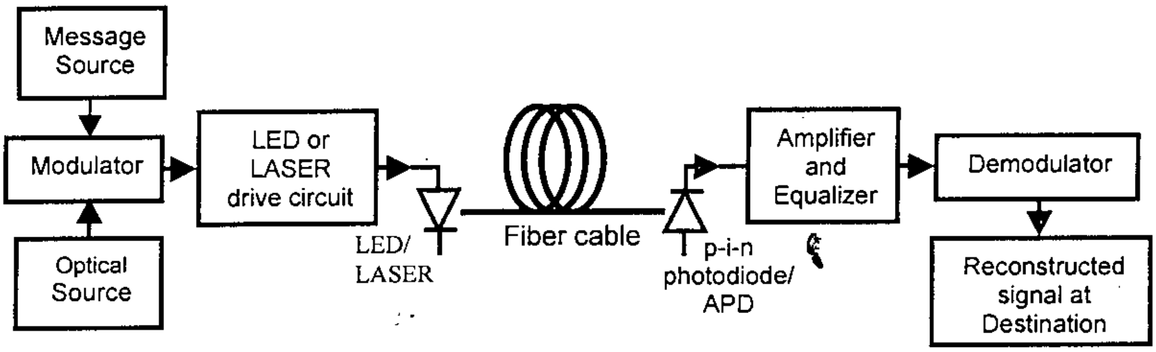

Figure 1.5: A typical optical fiber communication system

1.4 Fiber Characteristics

Signal attenuation (also known as 'fiber loss' or 'signal loss') is one of the most important properties of an optical fiber, because it determines the maximum repeaterless separation between transmitter and receiver. Fiber attenuation is important because a lightwave receiver requires at least a minimum amount of signal power to detect a transmitted bit with an acceptable error rate [3]. Of equal importance is the signal distortion in fiber, which causes optical signal pulses to broaden as they travel along the fiber. The signal distortion limits the information-carrying capacity of a fiber. These are the two principal factors to determine the optical transmission characteristics of fiber, which is shown in Figure 1.6. The total attenuation characteristics are shown in Figure 1.3.

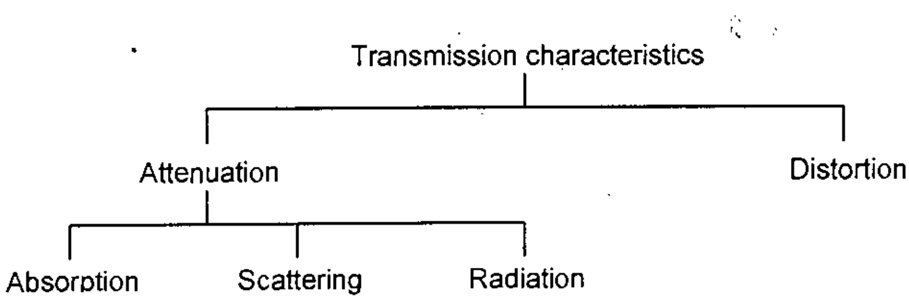

Figure 1.6: Parameters of fiber transmission characteristics.

Attenuation:

Signal attenuation in optical fiber stems from material composition, preparation and purification technique, and waveguide structure. The basic attenuation mechanisms can be categorized as material absorption, material scattering (linear and nonlinear scattering), curve and microbending losses, mode coupling radiation loss and loss due to leaky modes.

Absorption: Absorption is related to the material composition and the fabrication process for the fiber, which results in the dissipation of some of the transmitted optical power as heat in the waveguide. Absorption is caused by three different mechanisms:

(i) Absorption by atomic defects in the glass composition,

(ii) Intrinsic absorption by the basic constituent atoms of the fiber material,

(iii) Extrinsic absorption by impurity atoms in the glass material.

Scattering: Scattering phenomenon is of two types, namely, linear and nonlinear. Linear scattering mechanisms cause the transfer of some or all of the optical power contained within one propagating mode into a different mode. The transfer may be to a leaky or radiative mode, which does not continue to propagate but is radiated from the fiber. Linear scattering causes no change of frequency. There are two major types of linear scattering, namely, Rayleigh and Mie scattering.

Radiation: When the fiber is bent too much, the condition of total internal reflection may not be maintained and thus some of the light may leak through the cladding. This type of loss is known as macrobending loss where fibers are bent beyond the critical radius of curvature. There is maximum radius, below which no significant radiation occurs. There is another type of radiation loss termed as microbending loss, which occurs due to flaws and other imperfections of core.

Distortion:

Signal distortion occurs from the effect that the velocity of propagation of a light becomes frequency dependent in the fiber. This dependence is expressed by the following equation [4]

$$v_g = \frac{c}{n - \lambda \frac{dn}{d\lambda}} \tag{1.1}$$

Where v_g is the group velocity, n is refractive index of fiber medium, λ is wavelength of light and c is the light velocity. Thus different frequency components of the optical signal propagate at different velocities. The time delay between different spectral components causes spectral broadening of the optical pulses, and at the end of the fiber, the optical pulse broadens accordingly, as shown in Figure 1.7(a). This phenomenon is known as dispersion. After certain overlap, the adjacent pulses can no longer be individually distinguishable. This is known as intersymbol interference (ISI) as illustrated in Figure 1.7(b). Chromatic dispersion can severely limit the information capacity of an optical transmission system.

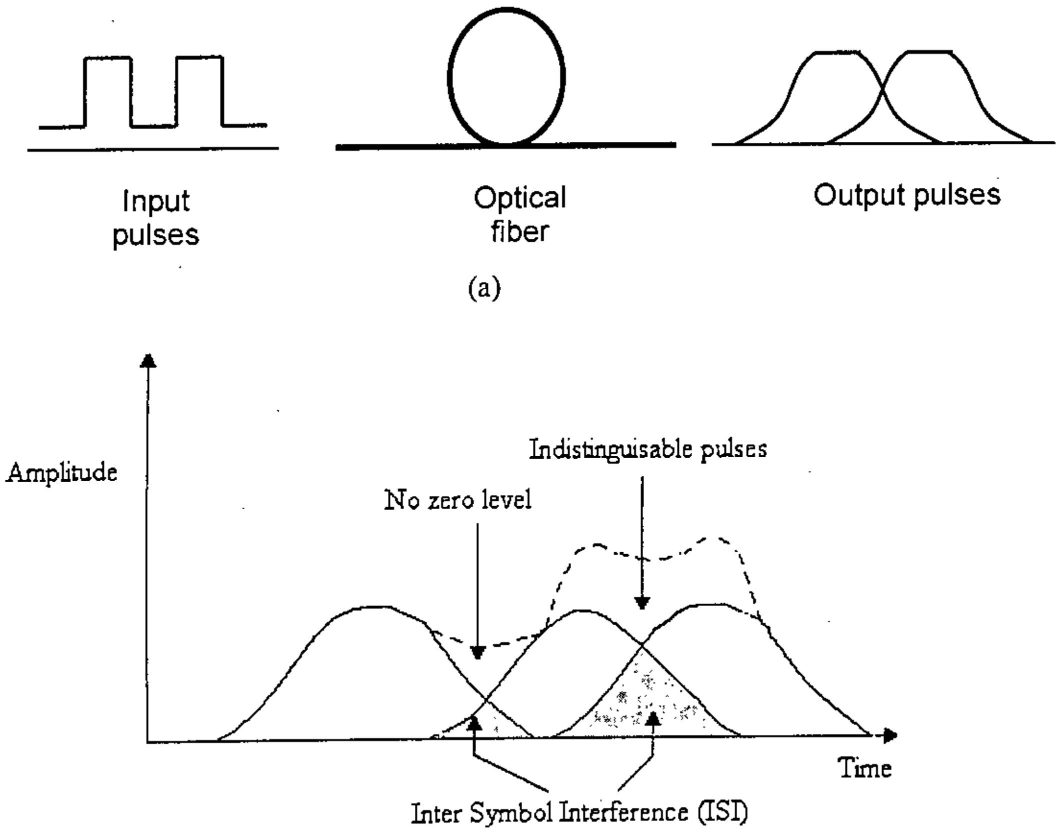

(b)

Figure 1.7: Effect of chromatic dispersion

Dispersion is of two types, namely, intermodal and intramodal. In multimode fiber, intermodal dispersion is due to the difference in propagation of various modes of the same signal. In single mode fiber, intramodal dispersion occurs within a single mode, because of group velocity being a function of wavelength, and this is generally known as chromatic dispersion. It has three components, namely, material dispersion, waveguide dispersion and polarization dispersion.

In multimode fibers, multipath dispersion that causes a severe limitation to the information capacity can be completely eliminated by reducing the core diameter to something in the region of 10μm. In single-mode fiber (SMF), the total dispersion can be determined by combining material dispersion and waveguide dispersion, which can be added algebraically. The interaction of various contributions in the total dispersion of a standard single-mode fiber is shown in Figure 1.8. The fact that waveguide dispersion has opposite sign compared to the material dispersion is of considerable practical interest, which can be utilized to develop special fibers, such as,

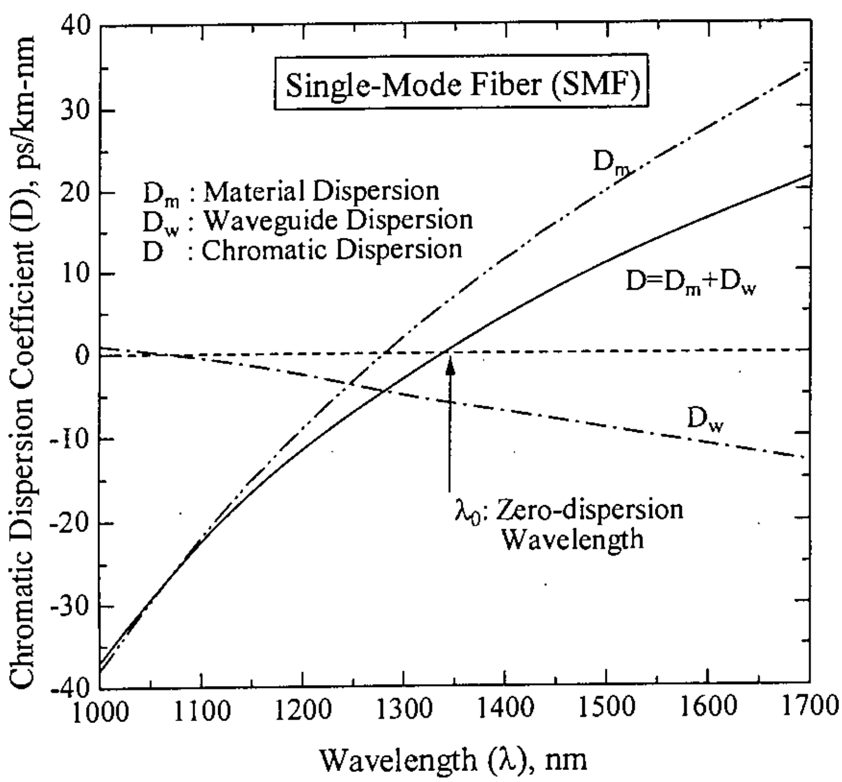

Figure 1.8: Chromatic dispersion characteristics of standard SMF [1].

dispersion flattened fiber (DF), dispersion shifted fiber (DSF) and nonzero dispersion shifted fiber (NZDSF) etc. The wavelength λ_0 is termed as the zero-dispersion wavelength, the wavelength at which dispersion is zero.

1.5 Background of this Study

Optical wavelength division multiplexing (WDM) systems using low dispersion fibers and erbium-doped fiber amplifiers (EDFA) are very attractive for future broadband information distribution networks. In principle, more than 1000 channels can be multiplexed at several gigahertzes intervals if fiber low dispersion region around 1.55μm (~ 12.5 THz bandwidth) is fully utilized [5]. WDM is one promising approach to exploit the huge bandwidth of optical fiber. WDM, the use of several distinct, separated wavelengths on a single-mode fiber, is revolutionizing the point-to-point optical links in the telecommunication industry. However these separate wavelengths are not truly independent but are coupled together by nonlinear interactions in fiber material. Fiber nonlinearities, such as, stimulated Raman scattering (SRS), stimulated Brillouin scattering (SBS), cross-phase and self-phase modulation and FWM result in severe performance degradation of lightwave communication systems by limiting the system capacity, maximum allowable input power and span lengths [6]. Among these nonlinear processes, FWM is the dominant nonlinear effect that severely degrades the performance of a long-haul multichannel transmission system [6]-[12].

First and second generation lightwave systems used 0.85μm and 1.33μm wavelength regions respectively where fiber attenuation loss is considerably high. By controlling the material and waveguide dispersion, λ_0 can be shifted to the lowest loss wavelength for silicate glass fiber at 1.55μm to provide both low dispersion and the lowest attenuation loss fiber as shown in Figure 1.9. These are called DSF and are designed to allow much higher information rates. However channels allocated near 1550 nm in DSF are seriously affected by nonlinear effects mainly four-wave mixing (FWM). DSF enhances the efficiency of generation of FWM waves by reducing the phase mismatch among the copropagating channels naturally provided by the fiber dispersion [12]. Recent trends in the design of lightwave systems are to achieve high data rates with long spacing between repeater amplifiers in a chain require high optical power per channel to satisfy the signal-to-noise (SNR) requirements. Thus, for WDM systems with long repeater spacing, the simultaneous requirements of high launched power and low dispersion fibers lead to the generation of new waves by FWM [13], [14]. Several methods have been proposed to mitigate the effect of FWM crosstalk, namely, arrangement of transmission fiber dispersion to prevent phase matching [15], unequal channel spacing (US) scheme [16], repeated unequal channel spacing (RUS) scheme [17], a combination of US/RUS and dispersion compensation schemes [18], or polarization-maintaining fiber [19] to reduce FWM crosstalk, but all

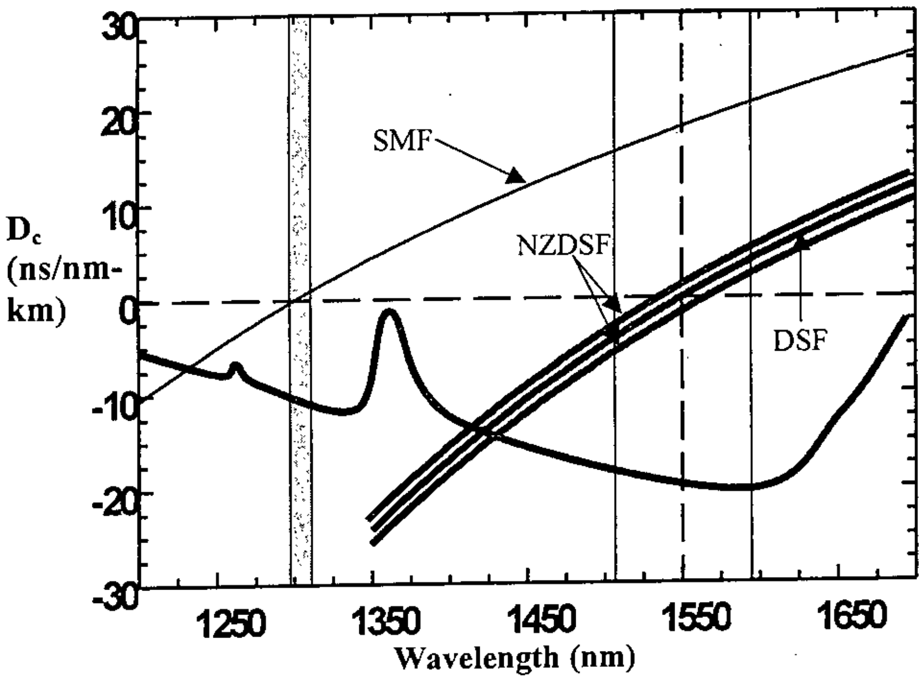

Figure 1.9: Chromatic dispersion and attenuation characteristics of various fibers [20]

these approaches cause some complexity and increase some difficulties of upgrading the system. Moreover, in US scheme the total bandwidth occupied by the all users expands drastically with the increase of number of channels, in RUS scheme total bandwidth requirement compared to US scheme is minimized but the BER performance is deteriorated due to FWM.

These have stimulated the development of new fiber designs, such as, NZDSF, in which λ_0 falls not exactly at 1550 nm but before or after 1550 nm and has low residual dispersion in the spectral window in which WDM and DWDM systems generally operate. These fibers are able to reduce FWM effect to some extent by maintaining the residual dispersion around 1550 nm wavelength and at the same time permit transmission at 10 Gbits/s over long distances. The transmission fibers are usually classified according to their dispersion characteristics. The dispersion curves for conventional non-dispersion shifted fiber (NDSF), DSF and NZDSF are shown in Figure 1.9. To avoid the FWM penalties in WDM systems NZDSF's are developed [21]. However, with the increase of number of channels, FWM crosstalk in NZDSF also increases and consequently system performance is again degraded.

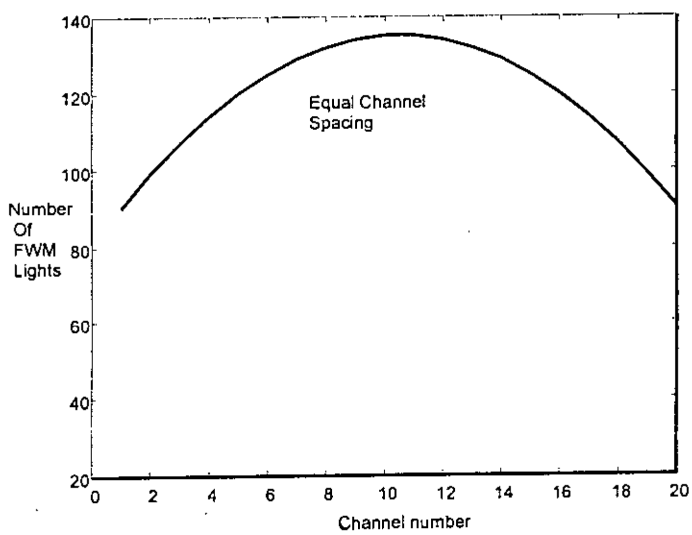

Figure 1.10: Number of FWM products at different channel positions [18]

Wavelength Shift Keying (WSK) is a new simple technique that can cancel the FWM crosstalk to first order [22]. It has been found that FWM spectrum is symmetric around the zero dispersion wavelength [18], [22]. By assigning the channels symmetrically around zero dispersion wavelength and using balanced detection, FWM crosstalk can be minimized significantly. The improvement of WSK-WDM system relative to conventional on-off WDM system has been studied without considering degenerate case, nonuniform dispersion and channel power depletion. The system performance may degrade at high launched power levels, because the propagating channels are depleted by power transferring to the mixing waves [23]. This problem can be solved by employing dispersion management scheme in which phase matching condition is disturbed by using fibers of different chromatic dispersion. The detailed performance analysis of WSK-WDM system considering FWM effect under various system limitations is yet to be reported.

1.6 Objective of this Study

The objective of this research is to study the performance of WSK technique in reducing the FWM effect in WDM optical network using an analytical approach. The effect of FWM interference on the system will be estimated. The system limitations for both conventional on-off WDM and WSK-WDM systems considering FWM effect will be evaluated and compared. The performance of both systems for different fibers, different number of channels, different channel spacing and for various transmission distances will be examined and compared. The performance of the proposed technique will also be compared to that of US and RUS schemes. Finally dispersion management scheme will be incorporated to the WSK system and then the improvement in the performance of this system will be assessed. Though this increases the system complexity, the achieved performance will compensate it satisfactorily. The results of this work are expected to contribute in the design of high-speed long-haul lightwave communication network with longer repeater spacing.

1.7 Thesis Outline

The thesis dissertation is composed of seven chapters.

Chapter 1 gives the introduction of fiber optic communication along with historical background. Recent developments in this field and the characteristics of optical fiber are also discussed. The background of this study and objective of this research work are addressed.

In chapter 2, different multichannel optical communication networks are described. The comparisons between WDM and FDM systems are also discussed.

In chapter 3, fiber nonlinearities and their impact on fiber optic communications are explained. The origin of FWM and its detrimental effect on multichannel transmission systems are characterized and analyzed elaborately with necessary mathematical models.

In chapter 4, system configuration of WSK-WDM system is presented. Estimation of four-wave mixing noise and its reduction process by WSK technique is explained. Bit error rate (BER), power penalty, allowable input power and the overall system capacity are evaluated for both conventional on-off WDM and WSK-WDM systems.

Chapter 5 describes the performance of WSK-WDM system in presence of FWM. The effects of different system parameters like number of channels, channel spacing, different types of fiber and fiber length on the system performance are also analyzed. The performance of WSK-WDM system is compared to that of conventional on-off WDM system and also compared to that of other FWM reduction techniques like US and RUS schemes.

Chapter 6 delineates the effect of chromatic dispersion on FWM efficiency. The dispersion management scheme using different nonuniform dispersive fibers is discussed. Then a combination of this scheme with WSK technique has been analyzed and the improvement of performance is compared to the previous results.

A brief conclusion along with suggestions for future works is addressed in chapter 7.

Chapter 2
OPTICAL COMMUNICATION NETWORK

2.1 Introduction

In this chapter different optical communication networks will be characterized. With the advance of fiber transmission techniques and optoelectronics, different optical multichannel communication systems have been evolved. Especially, the advent of semiconductor LASER with high gain and optical amplifier like erbium-doped fiber amplifier (EDFA) have created a stimulation to the multichannel optical communication networks.

2.2 Multichannel Communication Systems

The huge potential bandwidth of optical fiber can be efficiently utilized by multiplexing a number of channels and transmitting them through the fiber simultaneously. The transmission bandwidth of fiber is divided into a number of nonoverlapping frequency (or wavelength) bands and each of these bands is associated to support a single communication channel. Two principal kinds of multichannel systems are common in practical applications, namely, frequency division multiplexing (FDM) and wavelength division multiplexing (WDM). The Optical Time Division Multiplexing (OTDM) and Code Division Multiplexing (CDM) techniques are in under research. The first two schemes differ from each other in respect of transmitter/receiver configuration.

In the following subsections a short description on FDM and WDM systems will be given. In section 2.3, a comparative discussion between these two systems will be outlined.

2.2.1 Frequency Division Multiplexing (FDM)

In FDM the optical channel bandwidth is divided into a number of nonoverlapping frequency bands and each signal is assigned one of these bands of frequencies. The individual signal can be extracted from the combined signal by appropriate electrical filtering or optical filtering at the receiver terminal. Hence FDM is usually done

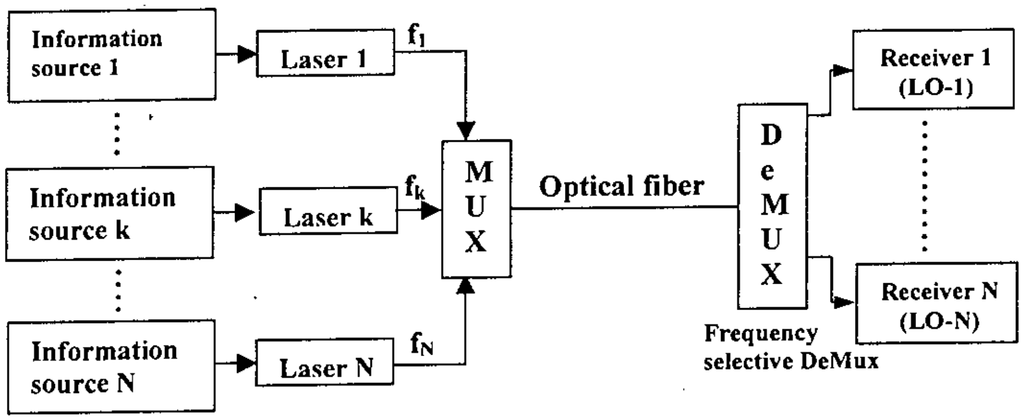

Figure 2.1: Optical FDM system

done electrically at the transmit terminal prior to intensity modulation of a single optical source. In case of broadcast communication, tunable optical filters or local oscillators (LO) can be used, and for point-to-point communication, fixed optical filters can be used. FDM is usually used for low capacity, short distance broadcast communications.

2.2.2 Wavelength Division Multiplexing (WDM)

WDM assigns incoming optical signals to specific wavelengths within the fiber (and EDFA) transmission bandwidth. Each of the wavelengths is launched into the fiber. The signals are demultiplexed at the receiving end and detected by the corresponding detector. There are different types of WDM setups, such as unidirectional and bidirectional setups.

Unidirectional WDM device is used to combine different signal carrier wavelengths onto a single fiber at one end and separate them onto their corresponding detectors at the other end.

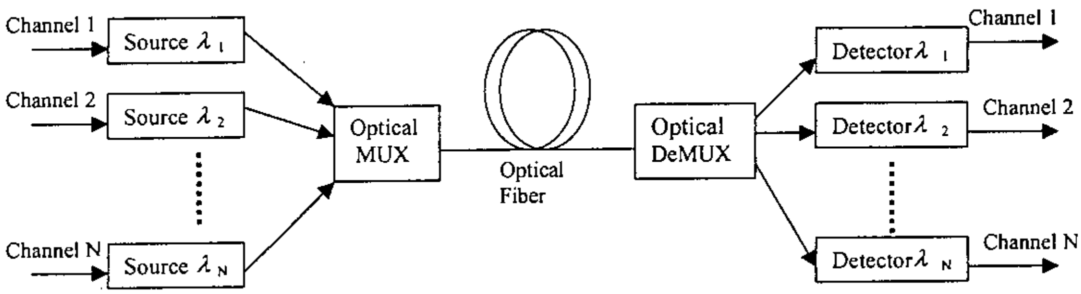

Figure 2.2: Block diagram of a unidirectional WDM network

The block diagram of a WDM network is shown in Figure 2.2. In the transmitting end there is a multiplexer using which a number of separate channels are fed to a single optical fiber. At the receiving end there is a demultiplexer, which separates the different channels and directs them to different receivers.

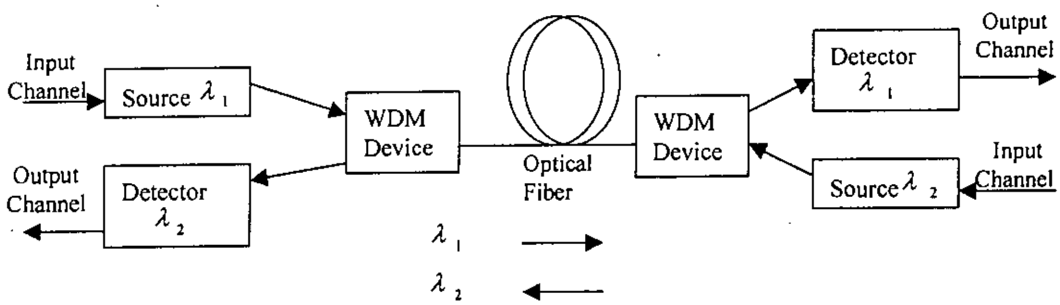

Figure 2.3: Block diagram of a bi-directional WDM system

In bidirectional WDM system two or more waves are transmitted simultaneously over the same fiber. It involves sending information in one direction at a wavelength λ_1 and simultaneously transmitting data in the opposite direction at a wavelength λ_2.

WDM system can further be categorized into two groups depending upon the wavelength separation between the adjacent channels. They are coarse WDM (CWDM) and dense WDM (DWDM). The WDM systems having channel spacing greater than 0.4 nm are generally known as CWDM, and those having channel spacing less than or equal to 0.4 nm are regarded as DWDM systems.

2.2.3 Dense Wavelength Division Multiplexing (DWDM)

The demand for communication and data transmission is growing rapidly due to increasing popularity of Internet and other multimedia applications. Optical transmission began to be used in trunk cables about 1990; the capacity of those systems was several hundred Mbits/s per fiber [24]. The capacity jumped to 2.5-5 Gbits/s with advent of high output semiconductor lasers and optical amplifiers in 1995. With the introduction of WDM technique for accessing the huge bandwidth of optical fiber, the system capacity is again increased to 10-20 Gbits/s. The overall transmission capacity now exceeds 100 Gbits/s per fiber due to improvement in fiber, optoelectronic devices and wavelength division multiplexing techniques [25]. Usually, those techniques are called dense WDM (DWDM).

The latest generation DWDM systems are capable of transmitting quantities of information at Tbits/s level and even higher. In DWDM system, the information carrying capacity of fiber is more effectively and efficiently utilized by using closely spaced channels. The channel spacing is more or less taken as equal to or less than 0.4 nm. Systems have been tested with 128 channels at 10 Gbits/s having 0.4 nm (50 GHz) channel spacing [26].

DWDM's most compelling advantages can be summarize as follows:

(1) *Transparency*: Because DWDM is a physical layer architecture, it can transparently support both time division multiplexed (TDM) and data formats such as ATM, Gigabit Ethernet, ESCON, and Fiber Channel with open interfaces over a common physical layer.

(2) *Scalability*: DWDM can leverage the abundance of dark fiber in many metropolitan area and enterprise networks to quickly meet demand for capacity on point-to-point links and on spans of existing SONET/SDH rings.

(3) *Dynamic provisioning*: Fast, simple, and dynamic provisioning of network connections give providers the ability to provide high bandwidth services in days rather than months.

DWDM has become the clear winner in the backbone. It was first deployed long haul routes at the time of fiber scarcity. Then the equipment savings made it the solution of choice for new long haul routes, even when ample fiber was available. While DWDM can relieve fiber exhaust in the metropolitan area, its value in this market extends beyond this single advantage. Alternatives for capacity enhancement exist, such as pulling new cable and SONET overlays, but DWDM can do more.

DWDM will continue to provide the bandwidth for large amounts of data. In fact, the capacity of systems will grow as technologies advance that allow closer spacing, and hence higher number of wavelengths. But DWDM is also moving beyond transport to become the basis of all-optical networking with wavelength provisioning and mesh-based protection. Switching at the photonic layer will enable this evolution, as will the routing protocols that allow light paths to traverse the network in much the same way as virtual circuits do today.

2.3 Comparison of WDM and FDM systems

Multiple channels are multiplexed in wavelength domain in WDM technique and in frequency domain in FDM technique. Optical WDM or FDM systems are highly promising for future broadband information transmission and distribution networks. Comparison between WDM and FDM networks are mentioned below:

1. In WDM systems wavelength spacing ($\Delta\lambda$) is small, in FDM system frequency spacing (Δf) is small.

2. In both cases point-to-point and broadcast communication are possible. But FDM is costly.

3. Both systems may have coherent or direct-detection receivers. But FDM requires optical/electrical filters/LO and WDM may employ optical filters or wavelength demultiplexers at the receiver. Wavelength demultiplexers can not be used for FDM.

4. In FDM systems huge loss of power occurs in the filters. On the other hand if wavelength demultiplexer is used in WDM receiver, then all the channels can be separated using a single unit without such losses.

5. WDM has simpler and cheaper receiver circuit.

2.4 Conclusion

A brief overview on different optical communication networks is presented in this chapter. Multiplexing techniques realize the great opportunity to utilize the huge available bandwidth of an optical fiber. Recent advances in the field of optics have created a way for practical implementation of WDM and FDM networks. Thus, these systems can meet the recent and future demand for high information rate.

Chapter 3
NONLINEAR PROCESSES IN FIBER

3.1 Introduction

With the increase of data rates on optical fiber, transmission lengths, number of channels, and optical power levels, nonlinear effects of fiber become dominant. The only worries that plagued the optical fiber in the early days were fiber attenuation and, sometimes, fiber dispersion; however, these issues are easily dealt with using newer fiber design having low attenuation and a variety of dispersion avoidance and cancellation techniques. Fiber nonlinearities present a new realm of obstacle to the high capacity, long haul multichannel optical communication systems that must be overcome.

3.2 Fiber Nonlinearities

The response of any dielectric material to the light becomes nonlinear for intense electromagnetic fields. Fundamentally, the origin of nonlinear response is related to the anharmonic motion of bound electrons under influence of an applied field. As a result, an intense light beam propagating through a fiber will induce a nonlinear polarization given by [27]

$$\mathbf{P} = \varepsilon_0 \left[\chi^{(1)} \cdot \mathbf{E} + \chi^{(2)} : \mathbf{EE} + \chi^{(3)} \vdots \mathbf{EEE} + \cdots \right] \tag{3.1}$$

which gives rise to nonlinear effects. Here ε_0 is the vacuum permittivity and $\chi^{(j)}$ ($j = 1, 2, \ldots$) is jth order susceptibility. The linear susceptibility $\chi^{(1)}$ represents the dominant contribution to $\boldsymbol{P}$. The second-order susceptibility is nonzero only for media that lack inversion symmetry at the molecular level. Since SiO_2 is a symmetric molecule, $\chi^{(2)}$ vanishes and optical fibers do not exhibit second-order nonlinear effects. The lowest order nonlinear effects in optical fiber originate from third-order susceptibility $\chi^{(3)}$, which is responsible for phenomena such as third-harmonic generation, four-wave mixing (FWM) and nonlinear refraction.

3.3 Origin of Nonlinear Effects

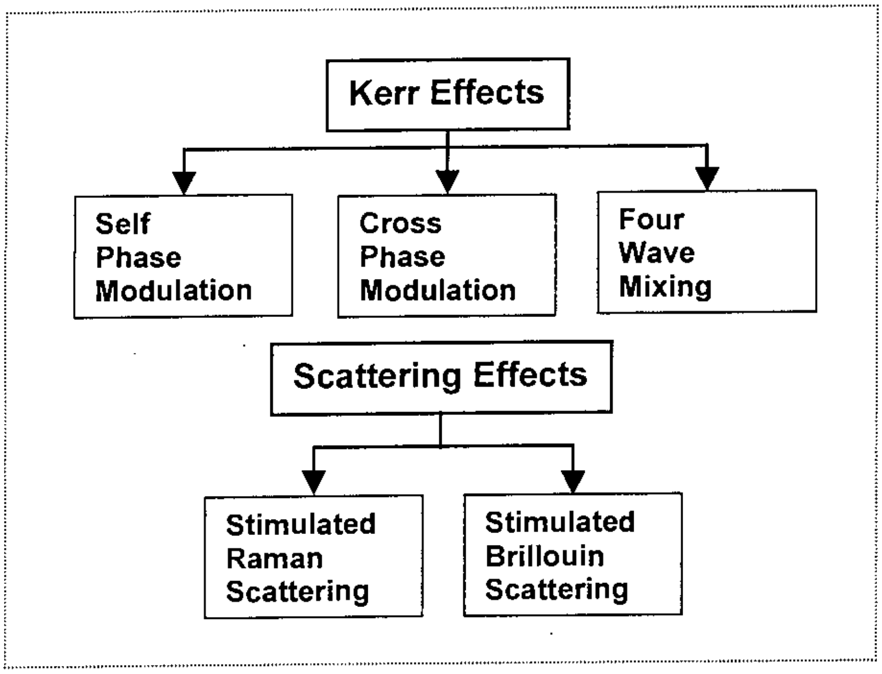

Figure 3.1: Nonlinear effects in fibers

Fiber nonlinearities arise from the two basic mechanisms. Firstly, most of the nonlinear effects in optical fibers originate from nonlinear refraction, a phenomenon that refers to the intensity dependence of refractive index of silica resulting from the contribution of $\chi^{(3)}$. The refractive index of fiber core can be expressed either as [27]

$$\tilde{n}(\omega,|E|^2) = n_0(\omega) + n_2|E|^2 \tag{3.2}$$

or as

$$n = n_0 + n_2\, P/A_{eff} \tag{3.3}$$

where n_0 is the linear part and n_2 is the nonlinear-index coefficient related to $\chi^{(3)}$ by the relation $n_2 = \frac{3}{8n}\mathrm{Re}(\chi^{(3)})$. P is the power of the light wave inside the fiber and A_{eff} is the effective area of fiber core over which power is distributed. The intensity dependence of refractive index of silica leads to a large number of nonlinear effects, such as, self-phase modulation (SPM), cross-phase modulation (XPM) and FWM.

The second mechanism for generating nonlinearities in fiber is the scattering phenomena. These mechanisms give rise to stimulated Brillouin scattering (SBS) and stimulated Raman scattering (SRS). Fiber nonlinearities that now must be considered in designing state-of-the-art fiber optic systems may be categorized as Kerr effects, which include SPM, XPM, and FWM, and scattering effects that include SBS and SRS. Different fiber nonlinear effects are briefly narrated below.

3.4 Stimulated Brillouin Scattering (SBS)

Stimulated Brillouin scattering (SBS) may be defined as light modulation through thermal molecular vibrations within the fiber. Incident photon produces a phonon of acoustic frequency as well as a scattered photon, and thereby produces an optical frequency shift.

It manifests through the generation of a backward-propagating Stokes wave that carries most of the input energy down-shifted from the frequency of incident light wave by an amount determined by the nonlinear medium. The process of SBS can be described classically as a parametric interaction among the pump wave, the Stokes wave, and an acoustic wave. The phase matching condition for SBS be written as

$$\boldsymbol{k}_1 + \boldsymbol{k}_2 + \boldsymbol{k}_s = 0 \qquad (3.4)$$

$$\boldsymbol{k}_s = 0,\ \boldsymbol{k}_1 \cong -\boldsymbol{k}_2$$

where k_1 and k_2 are wave vectors of two optical fields involved and k_s is the momentum of acoustic phonon which is very small compared to the pump and Stokes waves, thus phase matching can occur only if the Stokes wave propagates in the backward direction. This indicates that frequency shift is a maximum in backward direction reducing to zero in forward direction.

SBS sets an upper limit on the amount of optical power that can be usefully launched into an optical fiber. The SBS effect has a threshold optical power (around 5 to 10mW). The power limitation for SBS effect is also shown in Figure 3.3. SBS threshold about 2 mW is experimentally observed at 1.52 μm in 30 km fiber [28]. When the SBS threshold is exceeded, a significant fraction of the transmitted light is redirected back to the transmitter. This results in a saturation of optical power that reaches the receiver, as well as problems associated with optical signals being reflected back into the laser. The SBS process also introduces significant noise into the system, resulting in degraded BER performance. As a result, controlling SBS is particularly important in high-speed transmission systems employing external modulators and continuous wave laser sources. It is also of vital importance to the transmission of 1550 nm-based CATV transmission, since these transmitters often have the very characteristics that trigger the SBS effect.

The SBS threshold is strongly dependent on the linewidth of the optical source with narrow linewidth sources having considerably lower SBS thresholds. SBS threshold increases proportionally as the optical source linewidth increases.

3.5 Stimulated Raman Scattering (SRS)

Similar to SBS except that a high frequency optical phonon rather than acoustic phonon is generated in the scattering process. In the interaction process, a part of incident light is converted to another optical beam at a frequency downshifted by an amount determined by the vibrational modes of the nonlinear medium (called Stokes frequency). The incident light acts as pump for generating the frequency-shifted radiation called the

Stokes wave. For intense pump waves, the Stokes wave grows rapidly inside the medium such that most of the pump energy appears in it.

In a quantum mechanical view, a photon of the incident light is annihilated to create an optical phonon at the Stokes frequency and another photon at a new frequency. The phase matching condition can be written as

$$k_1 + k_2 + k_s = 0 \tag{3.5}$$

where k_s is the wave vector of the optical phonon. There are virtually two directions in fiber, so k_1 and k_2 have either the same or opposite directions.

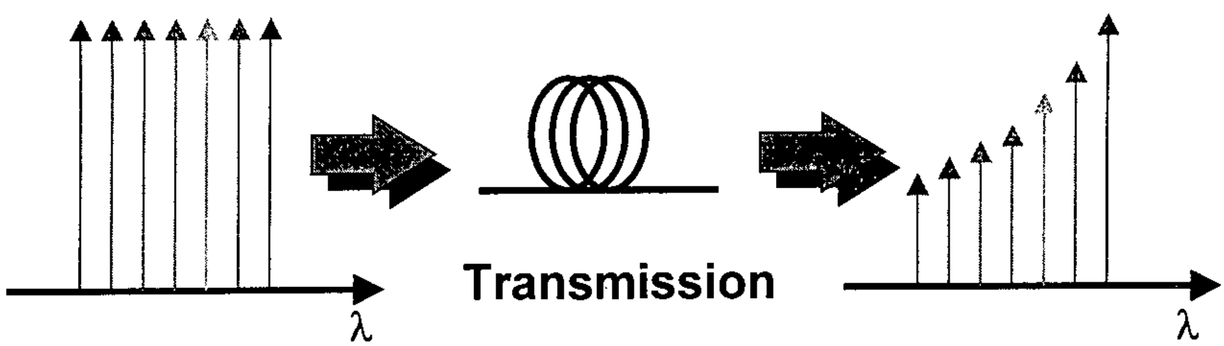

Figure 3.2: SRS effect in multichannel transmission system

Stimulated Raman scattering (SRS) is much less a problem than SBS, since its threshold (around 1 Watt) is nearly thousand times higher than SBS [29]. If the pump wave is increased beyond the threshold level, the scattering becomes stimulated and the pump wave losses its power to the Stokes wave. The pump wave is thus depleted due to SRS. In multichannel channel system, usually the effect first seen is that the shorter wavelength channels are robbed of power, and that power feeds the longer wavelength channels. That is, the lower frequency channels will be amplified at the expense of the higher frequency channels. The injected power to the lower frequency channels is not any spontaneous noise but from the transmitting power of a higher frequency user. Thus the Raman scattering process impairs the system performance at much lower optical powers for large number of channels. Figure 3.3 shows the maximum power limit imposed by SRS in a system with the mentioned parameters.

3.6 Self-Phase Modulation (SPM)

Self-phase modulation (SPM) is due to the power dependence of the refractive index of the fiber core. SPM refers the self-induced phase shift experienced by an optical field during its propagation through the optical fiber; change of phase shift of an optical field is given by [27]

$$\phi = (n + n_2|E|^2)k_0 L = \phi_L + \phi_{NL} \tag{3.6}$$

where $k_0 = 2\pi/\lambda$ and L is fiber length. ϕ_L is the linear part and ϕ_{NL} is the nonlinear part that depends on intensity. ϕ_{NL} is the change of phase of the optical pulse due to the nonlinear refractive index and is responsible for spectral broadening of the pulse. Thus different parts of the pulse undergo different phase shifts, which gives rise to chirping of the pulses. The SPM-induced chirp affects the pulse broadening effects of dispersion.

SPM interacts with the chromatic dispersion in the fiber to change the rate at which the pulse broadens as it travels down the fiber. Whereas increasing the dispersion will reduce the impact of FWM, it will increase the impact of SPM. As an optical pulse travels down the fiber, the leading edge of the pulse causes the refractive index of the fiber to rise causing a blue shift. The falling edge of the pulse decreases the refractive index of the fiber causing a red shift. These red and blue shifts introduce a frequency chirp on each edge, which interacts with the fiber's dispersion to broaden the pulse.

3.7 Cross Phase Modulation (XPM)

Cross phase modulation (XPM) is very similar to SPM except that it involves two pulses of light, whereas SPM needs only one pulse. In Multi-channel WDM systems, all the other interfering channels also modulate the refractive index of the channel under consideration, and therefore its phase. This effect is called Cross Phase Modulation (XPM).

XPM refers the nonlinear phase shift of an optical field induced by copropagating channels at different wavelengths; the nonlinear phase shift be given as [27]

$$\phi_{NL} = n_2 k_0 L(\underbrace{|E_1|^2}_{\text{SPM}} + \underbrace{2|E_2|^2}_{\text{XPM}}) \tag{3.7}$$

where $\boldsymbol{E}_1$ and $\boldsymbol{E}_2$ are the electric fields of two optical waves propagating through the same fiber with two different frequencies.

In XPM, two pulses travel down the fiber, each changing the refractive index as the optical power varies. If these two pulses happen to overlap, they will introduce distortion into the other pulses through XPM. Unlike, SPM, fiber dispersion has little impact on XPM. Increasing the fiber effective area will improve XPM and all other fiber nonlinearities.

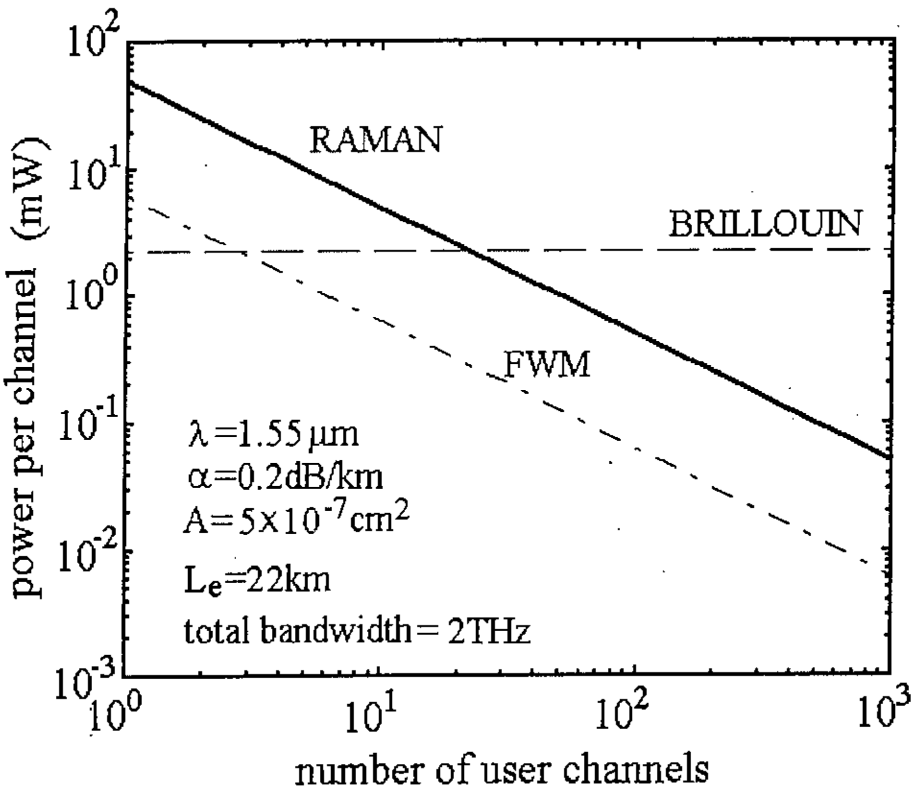

Figure 3.3: Maximum power per channel versus number of channels which ensures system deformation below 1dB for all channels in the case of SRS, SBS and FWM [22]

3.8 Four-Wave Mixing (FWM)

In the stimulated scattering processes, the optical fiber acts as a nonlinear medium and plays an active role through the participation of molecular vibrations. In many nonlinear phenomena the fiber plays a passive role except for mediating the interaction among several optical waves through a nonlinear response of bound electrons. Such processes are referred to as the parametric processes as they originate from light-induced modulation of a medium parameter such as refractive index. Nonlinear phenomena like harmonic generation, four-wave mixing and parametric amplification fall into this category. Since FWM effect in optical communication system is the main concern of this research work, the details of this effect are described in the following sub-sections.

3.8.1 Origin of FWM

Four-wave mixing (FWM) is caused by the nonlinear nature of the refractive index of optical fiber itself. And nonlinear refractive index of fiber depends on the intensity of propagating light. FWM effect is usually only observed in fiber optic communication systems with multiple channels. FWM is a third-order parametric process in which three waves of frequencies f_i, f_j and f_k interact through third-order susceptibility $\chi^{(3)}$ of fiber material and generate a fourth wave of frequency $f_{ijk} = f_i + f_j - f_k$ [14].

The origin of FWM can be understood by considering the third order polarization term given as [27]

$$\vec{P}_{NL} = \varepsilon_0 \chi^{(3)} \vdots \vec{E}\vec{E}\vec{E} \tag{3.8}$$

where $\boldsymbol{E}$ is the electric field, $\boldsymbol{P}_{NL}$ is the induced nonlinear polarization and ε_0 is the vacuum permittivity. Let us consider four optical waves oscillating at frequencies ω_1, ω_2, ω_3 and ω_4 respectively linearly polarized along the same axis x. The total electric field can be written as

$$\vec{E} = \hat{x}\frac{1}{2}\sum_{j=1}^{4} E_j \exp[i(k_j z - \omega_j t)] + c.c. \tag{3.9}$$

where $k_j = n_j\omega_j/c$, n_j is the refractive index and all four waves are assumed to be propagated in the same direction z. If we substitute (3.9) in (3.8) and express $\boldsymbol{P}_{NL}$ in the form

$$\vec{P}_{NL} = \hat{x}\frac{1}{2}\sum_{j=1}^{4} P_j \exp[i(k_j z - \omega_j t)] + c.c. \tag{3.10}$$

we find that P_j for j = 1- 4 consists of a large number of terms involving the products of three electric fields. For example P_4 can be expressed as

$$P_4 = \frac{3\varepsilon_0}{4}\chi^{(3)}_{xxxx}\{[|E_4|^2 + 2(|E_1|^2 + |E_2|^2 + |E_3|^2]E_4 + 2E_1E_2E_3\exp(i\theta_+) + 2E_1E_2E_3\exp(i\theta_-) + ...\} \tag{3.11}$$

where

$$\theta_+ = (k_1 + k_2 + k_3 - k_4)z - (\omega_1 + \omega_2 + \omega_3 - \omega_4)t \tag{3.12}$$

$$\theta_- = (k_1 + k_2 - k_3 - k_4)z - (\omega_1 + \omega_2 - \omega_3 - \omega_4)t \tag{3.13}$$

The term proportional to E_4 is responsible for SPM and XPM effects. The remaining terms are responsible for FWM. How many of these are responsible for a parametric coupling depends on the relative phase between E_4 and P_4 given by θ_+ and θ_- or a similar angle. FWM process becomes significant only if the relative phase nearly vanishes. This requires matching of the frequencies as well as the wave vectors. The latter requirement is often referred to as phase matching. In quantum mechanical terms FWM occurs when photons from one or more waves are annihilated and new waves are created at new frequencies such that the net energy and momentum are conserved during the parametric interaction. The main difference between the parametric processes and the scattering processes is that phase matching condition is automatically satisfied for the scattering processes as a result of the active participation of the nonlinear medium. By contrast the phase matching condition requires a specific choice of frequencies and the refractive indices for a parametric process like FWM to occur.

There are two types of FWM terms in Equation (3.11). The second term of the right hand side corresponds to the case in which three photons transfer energy to a single photon at the frequency $\omega_4 = \omega_1 + \omega_2 + \omega_3$. This term is responsible for phenomenon such as third harmonic generation when $\omega_1 = \omega_2 = \omega_3$ or frequency conversion to the wave at $2\omega_1 + \omega_3$ when $\omega_1 = \omega_2 \neq \omega_3$. In general it is difficult to satisfy the phase matching condition for such processes to occur in optical fibers with high efficiencies. The last term in Equation (3.11) corresponds to the case in which two photons at frequencies ω_1 and ω_2 are annihilated with a simultaneous creation of two photons at frequencies ω_3 and ω_4 such that

$$\omega_1 + \omega_2 = \omega_3 + \omega_4 \tag{3.14}$$

The phase matching requirement for this process to occur is that $\Delta k = 0$, where

$$\begin{aligned}\Delta k &= k_3 + k_4 - k_1 - k_2 \\ &= (n_3\omega_3 + n_4\omega_4 - n_1\omega_1 - n_2\omega_2)/c\end{aligned} \tag{3.15}$$

It is relatively easy to satisfy $\Delta k = 0$ for the FWM process described by (3.14) and (3.15) in the particular case in which $\omega_1 = \omega_2$. This partially degenerate case has been studied almost exclusively in optical fibers. Physically it manifests in a way similar to stimulated Raman scattering (SRS). A strong pump wave at ω_1 create two sidebands located symmetrically at the frequencies ω_3 and ω_4 with a frequency shift given by

$$\Omega_s = \omega_1 - \omega_3 = \omega_4 - \omega_1 \tag{3.16}$$

where for definiteness it is assumed that $\omega_3 < \omega_4$.

As can be seen from Equation (3.16) that the effect of FWM resembles SRS. In fact the low frequency sideband at ω_3 and the high frequency sideband at ω_4 are referred to as Stokes and anti-Stokes bands in direct analogy with SRS. The partially degenerate FWM is also known as three-wave mixing as only three distinct frequencies are involved in the nonlinear process. But generally it is referred to as four-wave mixing, reserving the term three-wave mixing for the processes mediated by $\chi^{(2)}$.

3.8.2 Phase-Matching Condition

As mentioned in the previous section the parametric gain for FWM peaks when the net wave vector mismatch is close to zero. The wave vector mismatch k can be expressed in the form

$$k = \Delta k_M + \Delta k_W + \Delta k_{NL} = 0 \tag{3.17}$$

where Δk_M, Δk_W and Δk_{NL} represent mismatching occurring as a result of material dispersion, waveguide dispersion and the nonlinear effects. For standard single mode fiber (SMF), significant amount of FWM can occur even when phase matching is not perfect to produce $k = 0$. The amount of tolerable wave vector mismatch depends on the relative magnitude of the fiber length L and the coherence length L_{coh}. Assuming that the contribution Δk_M dominates in Equation (3.17), the coherence length can be related to the frequency shift Ω_s and is given by [27]

$$L_{coh} = \frac{2\pi}{|\Delta k_M|} = \frac{2\pi}{|\beta_2|\Omega_s^2} \tag{3.18}$$

In the visible range typically β_2 = 50-60 ps^2/km resulting in $L_{coh} \geq 1km$ for frequency shifts $\nu_s = \Omega_s / 2\pi \leq 100$ GHz. Such large coherence lengths indicate that FWM can occur in SMF for frequency shifts such that $L \leq L_{coh}$.

3.8.3 Impact of FWM

FWM process can be a serious limiting factor for long haul multichannel communication systems. Its effect increases with the increase of number of channels, power per channel and fiber length. FWM process becomes stronger when channel spacing is smaller and chromatic dispersion of fiber is low. With increase of demand for very high information rates, more and more number of channels have to be provided by WDM/DWDM systems with larger bandwidth and lower spacing, and all these channels have to be placed within the lowest attenuation window using DSF/NZDSF, consequently the FWM effect becomes the main concern of lightwave communication systems.

FWM process can degrade the system performance in two ways:

1) Because of the FWM process a large number of new signals are generated. The total number of FWM products because of the interaction of N number of channels is

$$\text{Total no. of FWM Products} = \tfrac{1}{2}\left(N^3 - N^2\right) \tag{3.19}$$

Some of these FWM waves may occupy the same position as the original signals and may degrade system performance by interference.

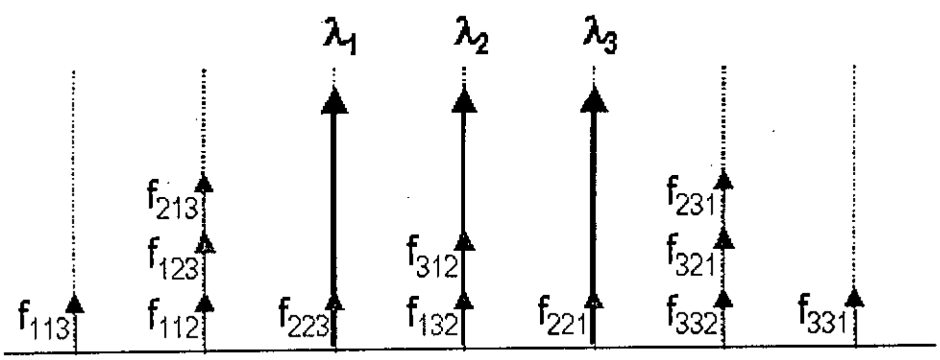

Figure 3.4: Interference caused by FWM products with original signals

Let us consider three channels as shown in Figure 3.4. Nine FWM products are generated here of which three falls on the original signal positions and interfere with them. With the increase of number of channels, the number of interfering products increases as shown in Figure 3.5.

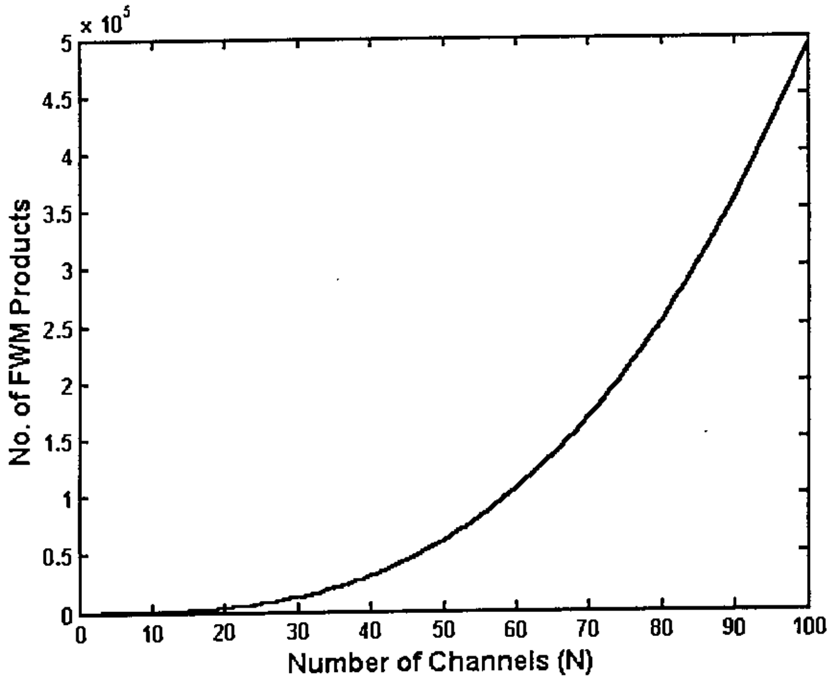

Figure 3.5: Number of FWM products as a function of number of transmitting channels

2) The second problem is that the new generated signals by FWM process take power from the original signals for their generation. As a result the original signals are depleted of power and becomes weaker [23]. Moreover, the distortion on the "1" bits is enhanced by the parametric gain provided by the channel power to the FWM waves at the detector [30].

3.8.4 Numerical Calculation of FWM

We have already mentioned that FWM is a third-order nonlinear parametric process in silica (glass), which is analogous to third-order intermodulation of radio systems [31], so that in a multichannel system, three optical frequencies mix through the third-order electric susceptibility of optical fiber to generate a fourth signal with frequency $f_{ijk} = f_i + f_j - f_k$, where f_i, f_j, and f_k ($k \neq i, j$) are the frequencies of three of the channels.

Thus, three copropagating waves give rise to nine new optical waves by FWM and in WDM system, this happens for every possible choice of three channels. In conventional WDM systems, the channels are typically equally spaced and this choice causes huge number of FWM products in the bandwidth of the system that may fall at the channel frequencies. The total number of FWM products can be calculated from Equation (3.19).

If we assume that the input signals are not depleted by the generation of mixing products, the power of the new optical signal generated at frequency f_{ijk} exiting the fiber is given by [12]

$$P_{ijk} = \frac{1024\pi^6}{n^4\lambda^2c^2}\left(\frac{D\,\chi_{1111}L_{eff}}{A_{eff}}\right)^2 P_iP_jP_ke^{-\alpha L}\eta \qquad (3.20)$$

where n is refractive index, λ is the wavelength of light, P_i, P_j and P_k are the input powers of three waves, D is the degeneracy factor, $D = 3$ for two-tone products ($f_i = f_j$) and $D = 6$ for three-tone products ($f_i \neq f_j$), χ_{1111} is nonlinear susceptibility and χ_{1111} = 4×10^{-15} esu and η is the mixing efficiency, A_{eff} is the effective area of the fiber and L_{eff} is the effective length of fiber, given by

$$L_{eff} = \frac{1}{\alpha}\left(1 - e^{-\alpha L}\right) \qquad (3.21)$$

with α as fiber attenuation loss. The third-order nonlinear susceptibility can be expressed in terms of nonlinear index of refraction n_2, in case of a single polarization, as

$$\chi_{1111}[esu] = \frac{cn^2}{480\pi^2}n_2[m^2/W] \qquad (3.22)$$

The mixing efficiency η is given by [12]

$$\eta = \frac{\alpha^2}{\alpha^2 + \Delta\beta^2}\left(1 + \frac{4e^{-\alpha L}\sin^2(\Delta\beta L/2)}{(1-e^{-\alpha L})^2}\right) \tag{3.23}$$

where $\Delta\beta$ is the propagation constant difference and be written as

$$\Delta\beta = \beta_{ijk} + \beta_k - \beta_j - \beta_i \tag{3.24}$$

Here β indicates the propagation constant. Efficiency η takes the maximum value of 1 for $\Delta\beta = 0$. In this situation the phase matching condition is satisfied. After expanding the propagation constant in a Tailor's series about zero-dispersion wavelength λ_0 and retain terms up to third order in ω–ω_0, the propagation constant difference $\Delta\beta$ representing the phase mismatch may be expressed as

$$\Delta\beta = (2\pi\lambda^2{}_0/c)(f_i - f_k)(f_j - f_k)\left[D_c + (\lambda_0{}^2/2c)(dD_c/d\lambda)\{(f_i - f_0) + (f_j - f_0)\}\right] \tag{3.25}$$

Here D_c is the fiber chromatic dispersion and f_0 is zero-dispersion frequency. For DSF, D_c $(f_0) = 0$.

To calculate the FWM crosstalk in a multichannel system, we assume N channels with same input p for each wavelength. The optical power generated by FWM at wavelength λ is given by

$$P_F(\lambda) = d^2C \sum_{\lambda=\lambda_i+\lambda_j-\lambda_k} P(\lambda_i)P(\lambda_j)P(\lambda_k) \tag{3.26}$$

where $P(\lambda_i)$, $P(\lambda_j)$ and $P(\lambda_k)$ are the fiber input power of three of the channels and if the input powers are equal, i.e. $P(\lambda_i) = P(\lambda_j) = P(\lambda_k) = P$, then Equation (3.26) can be written as

$$P_F(\lambda) = d^2 C \sum_{\lambda=\lambda_i+\lambda_j-\lambda_k} P^3 \tag{3.27}$$

and C is given by

$$C = \eta \kappa e^{-\alpha L} {L_{eff}}^2 \tag{3.28}$$

which is derived from Equation (3.19), where d is the degeneracy factor and $d = 1$ or 2 for $f_i = f_j$ or $f_i \neq f_j$ respectively, κ is fiber nonlinearity and is given as

$$\kappa = \frac{1024\pi^6}{n^4 \lambda^2 c^2} (3\chi_{1111})^2 \frac{1}{A_{eff}^2} \tag{3.29}$$

3.9 Conclusion

In this chapter, different fiber nonlinearities including scattering processes and parametric processes have been discussed. In last subsection we have illustrated the FWM effect in details, which is the main topic of this thesis. It has been observed that of all nonlinearities FWM is the most sensitive nonlinear effect that limits performance of multichannel lightwave communication systems. It is also found that many factors influence the FWM process, such as, number of channels, channel spacing, chromatic dispersion, fiber length, and core area.

With an increasing number of channels, the number of FWM waves generated grows rapidly. In addition, the decreased channel spacing results in more combinations having high mixing efficiency. Thus the FWM crosstalk increases as N^2. The critical power curve for a 1dB crosstalk limit from four-wave mixing is also drawn in Figure 3.3.

It can be seen from the figure that four-wave mixing imposes the most strict power limit upon the multichannel system with the given parameters. Furthermore, the nature of the FWM crosstalk (power depleted in bit 1s and noise generated in both bit 1s and 0s) results in an extremely high bit error rate (BER) in digital systems. Several FWM experiments have supported the theoretical predictions [9], [10], [32]. Thus four-wave mixing is the most sensitive to system parameters.

Simultaneous transmission of multiple wavelengths, increased signal powers and lower dispersion fibers all lead to the increased influence of four-wave mixing in present optical communication systems. To reduce the effect of FWM one has to consider many factors simultaneously. In the following chapter the characteristics of FWM crosstalk in WDM are studied and the reduction technique of FWM crosstalk will be investigated in details.

Chapter 4

WAVELENGTH SHIFT KEYING WDM SYSTEM

4.1 Introduction

Wavelength division multiplexing is recognized as the leading technology enabling a very large number of simultaneous connections within the large available bandwidth of a single fiber. In WDM systems that utilize low dispersion fibers and fiber amplifiers, the transmission performance is severely restricted by four-wave mixing. Different ways of mitigating the FWM effects have been proposed, including allocating unequally spaced channels, repeated unequal spaced channels, deploying dispersion managed fibers to prevent phase matching [15]-[18], or using polarization-maintaining fiber where polarization allocation schemes are employed to reduce FWM crosstalk [19]. All of these approaches increase system complexity. Wavelength shift keying technique is a simple scheme to depress FWM crosstalk. This technique is readily incorporated into the already existing WDM structure, and is especially advantageous to the systems that deploy low dispersion fibers.

4.2 Conventional on-off WDM system

In a conventional WDM system, each channel is assigned a particular wavelength, and N channels transmit their signals simultaneously on a same fiber. The system configuration is shown in Figure 4.1.

Narrow band optical sources provide power input for each channel, and they are modulated by on-off keying (OOK), that is, a certain amount of power is sent for bit 1 and no power is sent for bit 0 in the wavelength of that channel. An optical multiplexer couples the light from individual sources into a single fiber, where attenuation and spectrum deformation due to four-wave mixing occurs. At the receiving end, an optical demultiplexer separates the mixed signal into N receivers. Erbium-doped fiber amplifiers

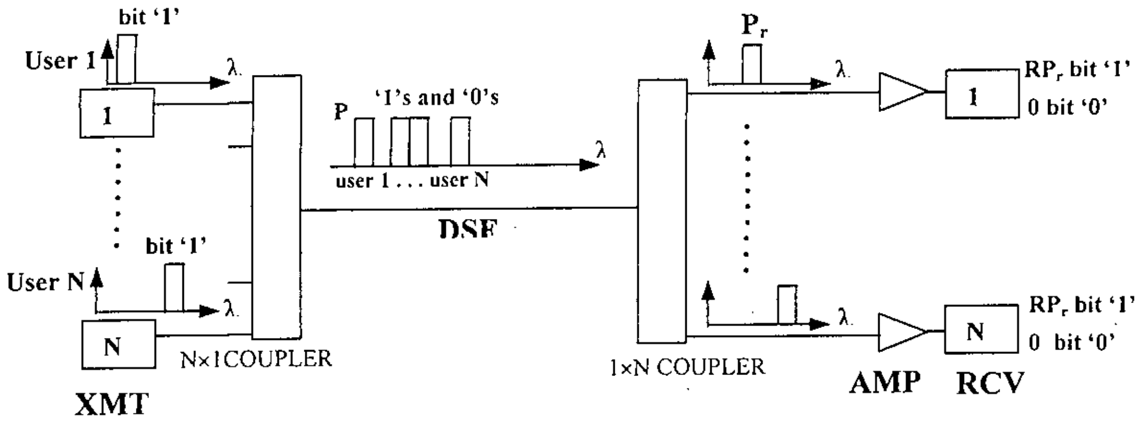

Figure 4.1: Diagram of a conventional on-off WDM system with *N* channels. XMT- transmitter, RCV - receiver, AMP -amplifier, DSF- dispersion shifted fiber.

are sometimes used as power amplifier and to pre-amplify the signals to compensate for the splitting loss. The received signal at the receiver in channel *i* is

$$Z_i = \begin{cases} RP_r & bit \ "1" \\ 0 & bit \ "0" \end{cases} \tag{4.1}$$

where *R* is the photodiode's responsivity: the ratio of the output current to its optical input power. P_r is the effective signal power received and be expressed as

$$P_r = L_r P \, e^{-\alpha L} \tag{4.2}$$

where *P* is the power output from the transmitter, or the input power to the fiber, and L_r is the insertion loss, α is attenuation constant and *L* is fiber length.

4.2.1 Evaluation of the Effects of FWM of Conventional WDM System Evaluation of Bit Error Rate, Power Penalty and Allowable input power

The numerical calculation of four-wave mixing noise and hence performance evaluation of repeaterless conventional on-off WDM system is presented in this subsection. Three types of noises, such as, thermal noise, shot noise, and FWM noise are considered and also assumed that all these noises have Gaussian distribution. It is assumed that lights from all optical sources have an identical state of polarization, which corresponds to considering the worst case situation for system degradation. The effect of laser phase noise can be ignored assuming the laser spectrum linewidth is narrow enough compared to modulation frequency and for simplicity polarization mode dispersion is ignored.

The probability of error or bit error rate (BER) is given by [33]

$$P_e = Q\left(\frac{\langle S^m\rangle - \langle S^s\rangle}{\sigma_m + \sigma_s}\right) \tag{4.3}$$

where σ is square root of noise power for bit '1' and bit '0' respectively; Q is complementary error function or co-error function and is expressed as

$$Q(x) = \frac{1}{\sqrt{2\pi}} \int_x^{\infty} \exp\left(-\frac{t^2}{2}\right) dt \tag{4.4}$$

where x is signal to noise ratio (SNR) and for conventional on-off WDM system the x is given by [32]

$$x = \frac{RP_r - R\left\{\frac{1}{8}\sum_{I} P_{ijk} + \frac{1}{4}\sum_{II} P_{ijk}\right\}}{\sqrt{N_{FWM} + N_{th} + N_{sh}} + \sqrt{N_{th}}} \tag{4.5}$$

where N_{th}, N_{sh} and N_{FWM} are thermal noise, shot noise and FWM noise respectively, P_{ijk} is the FWM power and be given in Equation (3.19) and the thermal noise and shot noise are given as

$$N_{th} = \frac{4KTB_e}{R_L} \tag{4.6}$$

$$N_{sh} = 2qB_e RP_r$$

where B_e is the electrical bandwidth of the receiver, K is Boltzman's constant, T is temperature in Kelvin, R_L is the terminating load resistance of the receiver, and R is photodetector's responsivity and be given as $R = \frac{\eta_q q}{hf}$ where η_q be quantum efficiency, q is the electron charge, h is the Planck's constant, f is operating frequency. The FWM noise is given by [32]

$$N_{FWM} = 2R^2 P_r \left\{ \frac{1}{8} \sum_{I} P_{ijk} + \frac{1}{4} \sum_{II} P_{ijk} \right\} \tag{4.7}$$

Where P_{ijk} is FWM power which is given by the Equation (3.19), summations I and II denote summation for $i \neq j \neq k$ and $i = j \neq k$ respectively; P_r is received power.

Now, the expression for power penalty for conventional IM/DD WDM system is derived. From Equation (4.5) and (4.7), using some approximation, the expression for received signal to achieve a given BER under FWM influence is deduced as (appendix A)

$$P_r = \frac{1}{R} \left(\frac{k_s + 2\sqrt{N_{th}}/x}{\frac{1}{x^2} - 2C_{im}^m} \right) \tag{4.8}$$

with $$C_{im}^m = \frac{1}{8} \sum_{I} \frac{P_{ijk}}{P_r} + \frac{1}{4} \sum_{II} \frac{P_{ijk}}{P_r} \tag{4.9}$$

where $N_{sh} = k_s R P_r$ with $k_s = 2qB_e$, and C_{im}^m is called the effective FWM crosstalk. The signal power to achieve a given BER without FWM is obtained from Equation (4.8) with $C_{im}^m = 0$ as

$$P_{r0} = \frac{x}{R}\left(x k_s + 2\sqrt{N_{th}}\right) \tag{4.10}$$

Now, the power penalty $P_p = P_r / P_{r0}$ at a given value of x_0 can be derived as (Appendix A)

$$P_p = \frac{1}{1 - 2x_0^2 C_{im}^m} \tag{4.11}$$

To determine the allowable input power, the above Equation is used and the expression is derived as

$$P = \left[\left(1 - \frac{1}{P_p} \right) \frac{P_r^p}{2x_0^2 C_{im}^{mp}} \right]^{\frac{1}{2}} \tag{4.12}$$

where $P_r^p = P_r / P$ and $C_{im}^{mp} = \frac{P_r}{P^3} C_{im}^m$.

4.3 Wavelength Shift Keying WDM System

It has been found that FWM spectrum is symmetric around the zero dispersion wavelength [18]. By assigning the channels symmetrically around the zero dispersion wavelength and using balanced detection at the receiver, FWM crosstalk can be minimized significantly. In WSK-WDM system, each user is assigned two specific wavelengths symmetric with respect to zero dispersion wavelength. One wavelength is used to transmit the bit '1' and the other is used to transmit the bit '0'. The modulated signals of all users are multiplexed and transmitted through the long haul low dispersion fibers and experience attenuation and spectral deformation due to four-wave mixing. At the receiver, two narrow band filters of each user select the two wavelengths and finally, they are demodulated by balanced receiver. The received signal of one wavelength of a user is positive for bit '1' and of other wavelength is negative for bit '0'. Erbium doped fiber amplifiers may be used as power amplifier and to pre-amplify the signals to compensate for the splitting loss. The received signal at the receiver in channel i is

$$Z_i = \begin{cases} RP_r & bit \ "1" \\ -RP_r & bit \ "0" \end{cases} \tag{4.13}$$

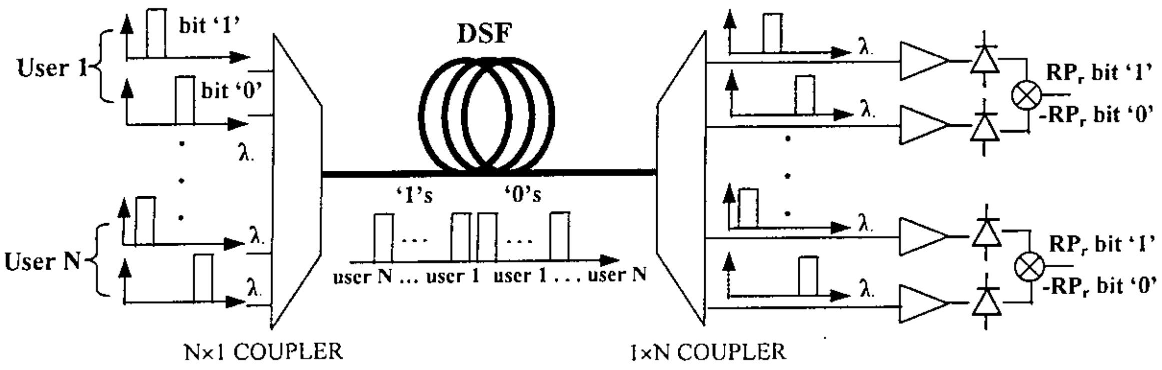

Figure 4.2: Schematic diagram of WSK-WDM system with N users

WSK requires twice as many wavelengths as conventional WDM to support a given number of users. But it has several advantages over on-off keying technique. The balanced detection yields 3 dB signal to noise advantage over single detection of on-off keying; higher data rates and higher allowable launched power can be achieved. For N users, $2N$ wavelengths are required for WSK model and N wavelengths are needed for WDM system. The schematic diagram of WSK-WDM system is shown in Figure 4.2.

4.3.1 Evaluation of the Effects of FWM of WSK-WDM System

Evaluation of Bit Error Rate, Power Penalty and Allowable input power

In WSK-WDM system, two lasers of each user are intensity modulated at two different wavelengths, which are symmetric around λ_0 and these are multiplexed with other channels and transmitted through the same fiber. At the balanced receiver, two wavelengths of each user are selected by two filters; one will select the wavelength that corresponds to bit '1' and the other for bit '0'. At the output of one filter, the field intensity of the optical signal is [34]

$$E^m = B_m \sqrt{P_r}\, e^{j\theta_r} + \sum_{ijk} B_i B_j B_k \sqrt{P_{ijk}}\, e^{j\theta_{ijk}} \tag{4.14}$$

where P_r is the received power of selected light, the summation term $\sum_{ijk} = \sum_{I} + \sum_{II}$ contains the summations *I* and *II* that denote summation for $i \neq j \neq k$ and $i = j \neq k$ respectively, P_{ijk} and θ_{ijk} are power and phase of those FWM lights generated from a channel combination of *i*-, *j*-, and *k*th channels that satisfy $f_{ijk} = f_i + f_j - f_k$ and $B_p = 1$ or 0 when *p*th channel is at the mark or space ($p = i, j, k$) respectively. $B_m = 1$ or 0 for mark or space, respectively. The output light of other filter is

$$E^s = B_s \sqrt{P_r}\, e^{j\theta_{ijk}} + \sum_{ijk} B_i B_j B_k \sqrt{P_{ijk}}\, e^{j\theta_{ijk}} \tag{4.15}$$

where $B_s = 0$ or 1 for mark or space, respectively.

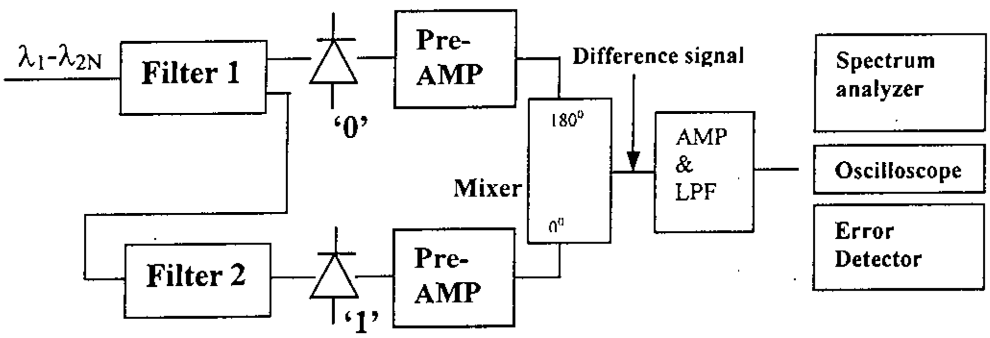

Figure 4.3: Balanced receiver configuration for single user in WSK-WDM system

The output from the two filters is detected by dual p-i-n photodiodes, and the signal current from the detectors, *S*, is written as [34]

$$S = R\left|E^m\right|^2 - R\left|E^s\right|^2$$

$$S = R\left[P_r\,(B_m - B_s) + 2\left\{B_m \sum_{ijk} B_i B_j B_k \sqrt{P_r\,P_{ijk}}\cos(\theta_r - \theta_{ijk}) - B_s \sum_{ijk} B_i B_j B_k \sqrt{P_r\,P_{ijk}}\cos(\theta_r - \theta_{ijk})\right\}\right]$$
$$+ R\left[\left|\sum_{ijk} B_i B_j B_k \sqrt{P_{ijk}}\,e^{j\theta_{ijk}}\right|^2 - \left|\sum_{ijk} B_i B_j B_k \sqrt{P_{ijk}}\,e^{j\theta_{ijk}}\right|^2\right] + n_{th} + n_{sh} \tag{4.16}$$

where $R = \dfrac{\eta_q q}{hf}$, $\theta_{ijk} = \theta_i + \theta_j - \theta_k$ and n_{th} and n_{sh} are thermal noise and shot noise respectively. The detected signal level can be written as

$S =$

$$S^m = R\left\{P_r^m + P_F^m + 2\sqrt{P_r^m P_F^m}\cos(\theta_r^m - \theta_F^m)\right\} \quad \text{for "mark"} \tag{4.17}$$

$$S^s = -R\left\{P_r^s + P_F^s + 2\sqrt{P_r^s P_F^s}\cos(\theta_r^s - \theta_F^s)\right\} \quad \text{for "space"} \tag{4.18}$$

here P_F and θ_F are same as P_{ijk} and θ_{ijk} ; 'm' denotes "mark" and 's' denotes "space". It can be assumed that $P_r^m = P_r^s$ and $P_F^m = P_F^s$. Then Equation (4.16) can be written as

$$S = R\left[P_r\,(B_m - B_s) + 2\left\{B_m \sum_{ijk} B_i B_j B_k \sqrt{P_r\,P_F}\cos(\theta_r - \theta_F) - B_s \sum_{ijk} B_i B_j B_k \sqrt{P_r\,P_F}\cos(\theta_r - \theta_F)\right\}\right]$$
$$+ R(P_F - P_F) + n_{th} + n_{sh} \tag{4.19}$$

It is evident that the average FWM power becomes nil, i.e. first order FWM crosstalk is cancelled out. So, in WSK-WDM system there is no first order FWM interference, higher order FWM products may exist.

Signal levels S^m and S^s can take various random values. In general, the probability distribution of a variable composed of independent random variables can be considered to have a Gaussian profile whose mean value and variance are the summation of the mean values and variance of the individual random variables. That is, the signal level has Gaussian probability distribution, the mean values are

$$\langle S^m \rangle = RP_r \quad \text{for "mark"} \tag{4.20}$$

and

$$\langle S^s \rangle = -RP_r \quad \text{for "space"}$$

The variances are

$$\sigma_m^2 = \sigma_F^{(m)2} + N_{th} + N_{sh} \qquad \text{for "mark"} \tag{4.21}$$

with $\sigma_F^{(m)2} = 2R^2 P_r \left\{ \frac{1}{8} \sum_I P_{ijk} + \frac{1}{4} \sum_{II} P_{ijk} \right\}$ (4.22)

and $\sigma_s^2 = \sigma_F^{(s)2} + N_{th} + N_{sh}$ for "space" (4.23)

with $\sigma_F^{(s)2} = 2R^2 P_r \left\{ \frac{1}{8} \sum_I P_{ijk} + \frac{1}{4} \sum_{II} P_{ijk} \right\}$ (4.24)

and $\sigma_F^{(m)2} \approx \sigma_F^{(s)2}$

where $\sigma_F^{(m)2}$ and $\sigma_F^{(s)2}$ are variances of FWM signal. Thus, the total signal variation has a Gaussian profile and the error probability P_e can be ascertained using Equation (4.3) and (4.4), but the SNR for this system is (Appendix B)

$$x = \frac{\langle S^m \rangle - \langle S^s \rangle}{\sigma_m + \sigma_s}$$

$$= \frac{RP_r}{\sqrt{N_{FWM} + N_{th} + N_{sh}}} \tag{4.25}$$

where $N_{FWM} = \sigma_F^{(m)2} = \sigma_F^{(s)2}$

In WSK-WDM system, the decision statistic conforms to that of an antipodal system, Whereas, WDM system has a decision statistic of an orthogonal system. The bit error rate

(BER) of WSK-WDM system is then expressed as

$$P_e = Q(x) = \frac{1}{2} erfc\left(x / \sqrt{2} \right) \tag{4.26}$$

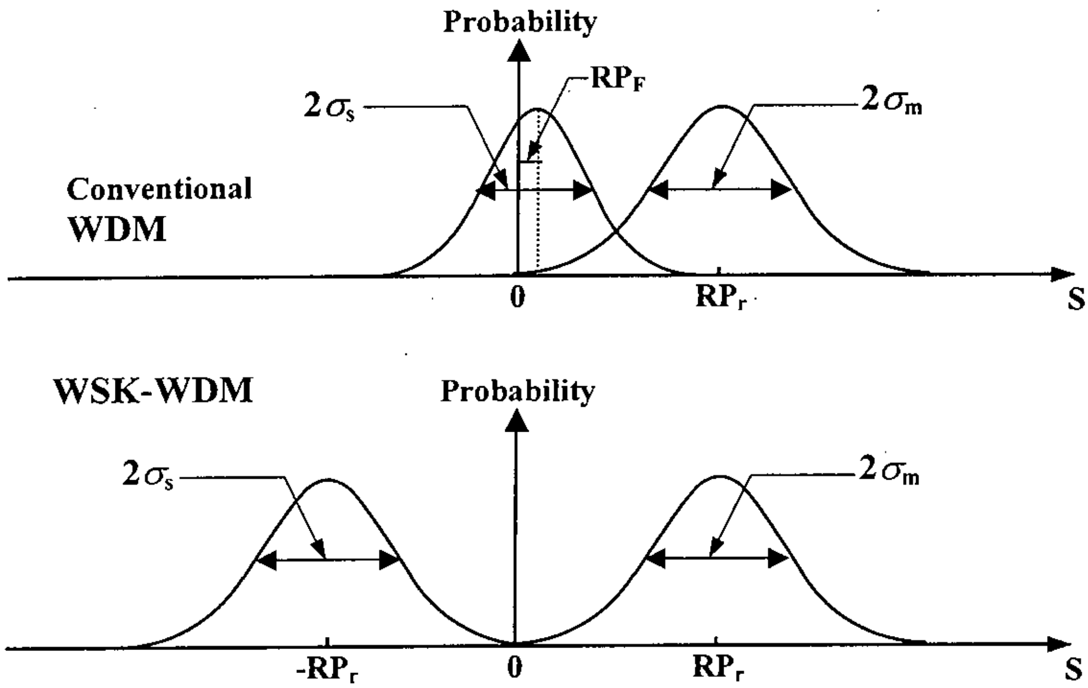

Figure 4.4: Decision statistic for conventional WDM and WSK-WDM systems

From Equations (4.24) and (4.25), the expression for received signal to achieve a given BER under FWM influence is

$$P_r = \frac{b \pm \sqrt{b^2 + 4ac}}{2a} \tag{4.27}$$

where $a = \frac{R^2}{x^2} - 2R^2 \frac{P^2}{P_r^p} C_{im}^{mp}$

$b = k_s R$

$c = N_{th}$

and $C_{im}^{mp} = \frac{P_r}{P^3} C_{im}^m$ with $C_{im}^m = \frac{1}{8} \sum_I P_{ijk} + \frac{1}{4} \sum_{II} P_{ijk}$

The signal power to attain a given BER without influence of FWM is

$$P_{r0} = \frac{b \pm \sqrt{b^2 + 4a^P c}}{2a^P} \tag{4.28}$$

where $a^P = \frac{R^2}{x^2}$ and b, c are as usual.

The power penalty of a system is already defined as the ratio of received power with FWM noise to the received power without the influence of FWM. Hence, The expression for power penalty for WSK-WDM system is derived as (Appendix C)

$$P_p = \frac{P_r}{P_{r0}} = \frac{(b + \sqrt{b^2 + 4ac})a^P}{(b + \sqrt{b^2 + 4a^P c})a} \tag{4.29}$$

The allowable input power is evaluated from the above formula and the expression for maximum allowable input power per channel for this system is deduced as (Appendix C)

$$P = \left[\frac{P_r^P}{2R^2 C_{im}^{mp}} \left\{ a^P - \frac{\left((b + \sqrt{b^2 + 4a^P c}) \left(\frac{P_p a}{a^P} \right) - b \right)^2 - b^2}{4c} \right\} \right]^{1/2} \tag{4.30}$$

where $P_r^P = \frac{P_r}{P} = L_r e^{-\alpha L}$

4.4 Conclusion

A detailed analysis of conventional on-off WDM and WSK-WDM systems in context of FWM process is presented in this chapter. The impact of FWM on the system performance is described both qualitatively and quantitatively.

Chapter 5

PERFORMANCE OF WSK-WDM SYSTEM

5.1 Introduction

The performance of a multichannel WSK-WDM transmission system in presence of FWM has been evaluated in this chapter. A repeaterless network with uniform chromatic dispersion is considered. The system performance dependence on various system parameters such as transmitting power per channel, number of channels, fiber length will be examined. Finally, the performance of WSK-WDM system is compared to that of other FWM reduction schemes like unequal channel spacing (US) and repeated unequal channel spacing (RUS).

5.2 Results

5.2.1 Bit Error Rate

The bit error rate (BER) performance of WSK-WDM and conventional on-off WDM systems using DSF is shown in Figure 5.1. The error probability of both systems is compared for 8-channel as a function of the signal power. The BER for both systems has been calculated considering only thermal noise, shot noise and FWM noise, all of which are assumed to have Gaussian distribution. The fiber and system parameters used in the calculations are listed in Table-1. The parameters are chosen for comparing a conventional equally spaced WDM system performance measuring with 8 channels [35].

The FWM power is proportional to the cube of transmitting power. At low signal power, the FWM noise is small compared to the shot noise and thermal noise and the performance is limited by these noises. As the signal power increases, the BER decreases. As signal power increases further, the FWM noise becomes dominant and the BER starts to increase. That is, the system is impaired by FWM interference and the performance is degraded for large power levels. For all power levels, the performance of WSK-WDM excels the conventional WDM system. The BER of conventional WDM is higher than 10^{-6} whereas for WSK-WDM system there is a signal power range within which BER is lower than 10^{-12} [22], [36]. In the calculation, 8 and 16 wavelengths are required for conventional WDM and WSK technique respectively to support 8 users. The channel spacing is 200 GHz (1.6 nm) in both cases.

Figure 5.2 shows the BER performance of both systems for 16 users. The channel spacing is 200 GHz. Figure 5.3 and 5.4 show the BER performance for both systems for the same data as mentioned above but for NZDSF. The effect of channel spacing on BER of WSK-WDM is illustrated in Figure 5.5. It's apparent that BER decreases with the increase of channel spacing.

Table-1: The fiber and system parameters used in the numerical calculations

Number of users	N	8, 16
Fiber Length	L	137 km
Attenuation	α	0.24 dB/km
Wavelength	λ	1.55 μm
Channel spacing	Δf	100 GHz, 200 GHz
Power penalty	P_p	0.7 dB
Fiber nonlinearity	κ	5.84×10‾6 $m^{-2}W^{-2}$
Responsivity	R	0.85 A/W
Bit Rate	B_r	10 Gbps
Dispersion (DSF)	D_c	0 ps/nm-km
Dispersion slope (DSF)	$\frac{dD_c}{d\lambda}$	0.055 ps/nm^2-km
Dispersion (NZDSF)	D_c	-2.0 ps/nm-km
Dispersion slope (NZDSF)	$\frac{dD_c}{d\lambda}$	0.07 ps/nm^2-km

5.2.2 Power Penalty

The power penalty suffered by both systems to achieve a BER of 10^{-9} is calculated and shown in Figure 5.6. Power penalty increases with input power per channel. From figure, it is obvious that for a given input power, WSK offers lower power penalty compared to conventional WDM counterpart [36].

5.2.3 Allowable Input Power

The allowable input power for a given power penalty of 0.7 dB at BER of 10^{-9} is estimated and shown in Figure 5.7 for various number of channels. WSK-WDM permits much higher allowable input power compared to that of conventional on-off WDM system even considering equal bandwidth [36].

5.2.4 Bit Rate-Distance Product

Allowable input power is determined for various transmission distances to achieve a BER of 10^{-9} for the bit rate of 2 Gbps limiting each system to the same total bandwidth, which is illustrated in Figure 5.8. It indicates that for a given BER of 10^{-9}, WSK-WDM gives longer repeater spacing.

Bit rate-distance product, which is the product of bit rate and transmission distances that allows a given BER i.e. a certain degree of signal clarity without signal regeneration, is another criterion for evaluating the performance of a communication system [37]. Setting the BER performance to 10^{-9}, certain number of channels is chosen and then fiber length is calculated the system can support. That is, we increase the fiber length until the lowest point on its performance curve lies exactly on the 10^{-9} BER line. We choose a bit rate of 2 Gbps, because for this bit rate, the maximum unrepeatered link length is limited by attenuation rather than dispersion. Using the parameters mentioned in Table 1 and in Table 2, for DSF the overall capacity is predicted to be 10.752 THz-km for WSK-WDM system, whereas for WDM system it is 4.96 THz-km, the improvement is 2.168 times.

The comparison is done considering that each system occupy the same total bandwidth. Figure 5.8 also reveals that WSK technique yields more bit rate-distance product.

Table-2: System parameters and Bit rate-distance comparison.

Parameters	Conventional WDM	WSK-WDM	Improvement in capacity
Bit Rate	2 Gbps	2 Gbps	2.168
BER	10^{-9}	10^{-9}	
Channel spacing	100 GHz	50 GHz	
No. of Channels	16	32	
Maximum repeater spacing	155 km	168 km	
Bit rate×distance	4.96 THz-km	10.752 THz-km	

5.3 Comparison with other FWM Reduction Schemes

In WDM system with equally spaced channels, a lot of product terms produced by the FWM process fall at the existing channel frequencies, giving rise to channel crosstalk and thereby severely degrade the system performance [10], [11]. Unequally spaced channel allocation (US or USCA) is one of the most attractive solutions, which can greatly reduce the FWM effect [16], [38]. In US scheme, the frequency separation between any two channels is different from that of any other pair of channels. If all the channel frequencies are allocated appropriately, no FWM lights will be generated at any of the existing channel frequencies, thereby suppressing the FWM crosstalk. The use of proper unequal channel spacing keeps FWM waves from coherently interfering with the signals. However, in US scheme, the total bandwidth occupied by all the signals, expands drastically with the increase of number channels. Thus, it is difficult to have a lot of channels in US scheme. But it is important to keep the total bandwidth as narrow as possible, as because, the frequency range of optical amplifier is limited. To overcome this problem, repeated unequally spaced (RUS) channels have been proposed and their effectiveness has been investigated [17]. RUS scheme is a periodic allocation of unequally spaced (US) channels, where a narrow bandwidth can be achieved even for a large number of users but at the cost of a few FWM lights, which coincident with the signal frequencies.

Wavelength shift keying is a new technique that can suppress the FWM products generated in the bandwidth of the system. The system configuration is already described. The BER performance of US scheme is much better than RUS or WSK scheme, since proper unequal channel allocation can eliminate all the FWM components that would interfere with the existing channels i.e. FWM crosstalk is nil. WSK-WDM system yields the lower error probability than that of RUS scheme, but the total bandwidth occupied by all the channels in WSK-WDM system to support the same number of users, is relatively large. These are illustrated in Table-3, Figure 5.9 and 5.10. WSK-WDM system yields BER of 10^{-13} and 10^{-11} for 8 and 10 users respectively using DSF, whereas RUS scheme provides 10^{-10} and 10^{-9} respectively. The US system does not suffer from FWM crosstalk. In this scheme, with the increase of signal power, BER decreases, i.e. probability of error keeps decreasing which is noted in Figures 5.9 and 5.10, and at a certain point it becomes zero ($P_e = 0$) for the reason that input power is sufficient to overcome the thermal noise and shot noise and there is no FWM crosstalk.

US channel allocation technique requires huge bandwidth for large number of channels, which is not desirable and feasible. There is hardly any other US channel slots for more than 10 users. Now, if we compare RUS channel allocation technique in WDM with WSK-WDM system, it is evident that the latter provides lower BER within a particular range of signal power but at the cost of increased bandwidth. If we limit the both schemes to the same total bandwidth, WSK-WDM gives BER of 10^{-7} for 10 users, which is 10^{-9} for RUS scheme, it is shown in Figure 5.11. From this figure, it is also noted that RUS scheme provides lower BER in the high power levels, but after a certain level WSK-WDM gives lower BER. On the other hand, at low power levels, WSK-WDM always provides lower error probability where thermal noise and shot noise dominate and FWM noise is comparatively small. So it is obvious that WSK-WDM is more noise tolerant than any of other two schemes.

Table 3: Parameters used in the calculations and the results obtained for comparison among US, RUS and WSK-WDM schemes

Parameters	WSK-WDM		RUS scheme		US scheme	
Minimum channel separation in no. of slots, n	---		5		5	
Channel spacing, Δf_c	125 GHz		125 GHz		125 GHz	
Bit rate, B_r	10 Gbps		10 Gbps		10 Gbps	
No. of channels	16	20	8	10	8	10
BW required	2000 GHz	2500 GHz	1025 GHz	1350 GHz	1400 GHz	2025 GHz
Minimum BER	10^{-13}	10^{-11}	10^{-10}	10^{-9}	$P_e = 0$	$P_e = 0$

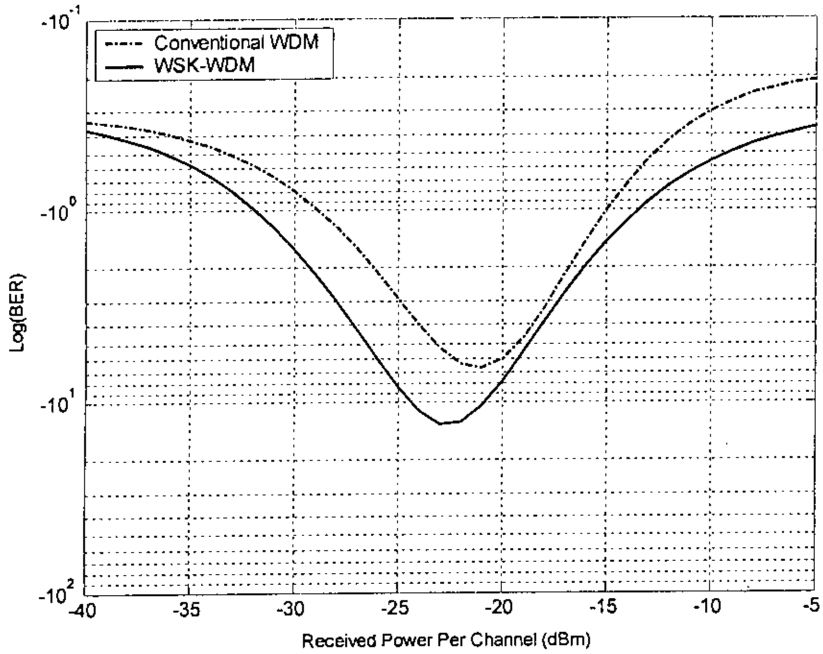

Fig 5.1: Error probability of WSK-WDM and conventional WDM systems as a function of received power per channel after transmission through 137 km of DSF supporting 8 users [22], [36]

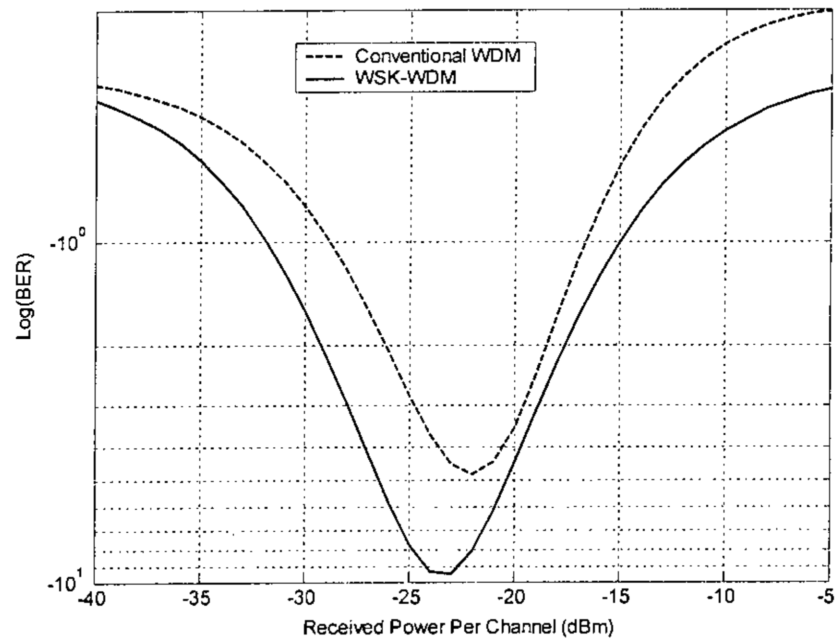

Fig 5.2: Error probability of WSK-WDM and conventional WDM systems as a function of received power per channel for DSF supporting 16 users

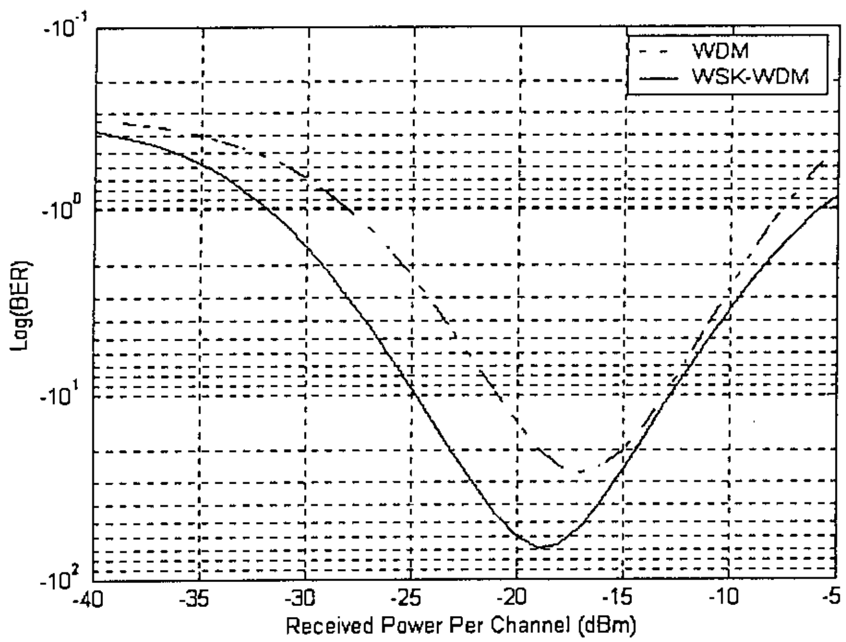

Fig. 5.3: Error probability of WSK-WDM and conventional WDM systems as a function of received power per channel after transmission through 137 km of NZDSF supporting 8 users

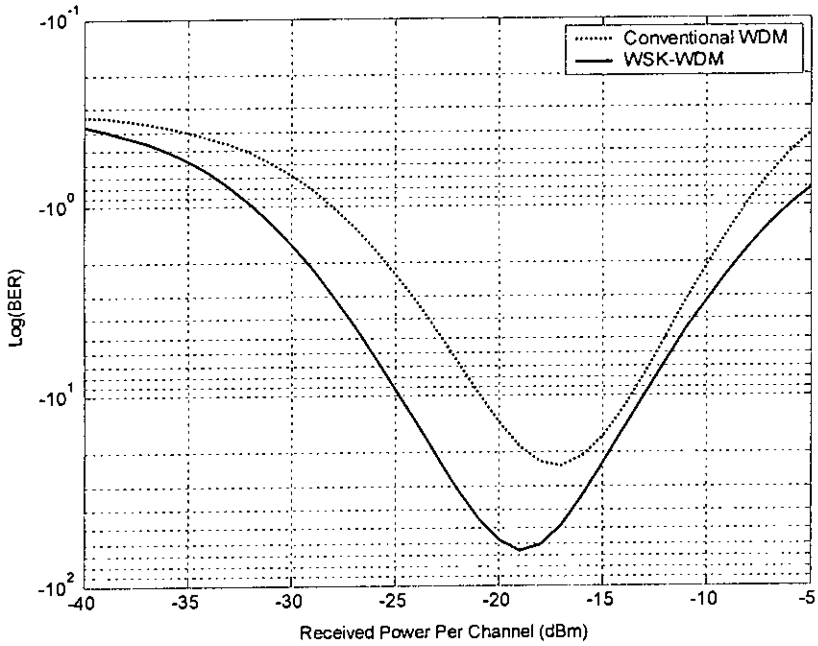

Fig. 5.4: Error probability of WSK-WDM and conventional WDM systems as a function of received power per channel for NZDSF supporting 16 users

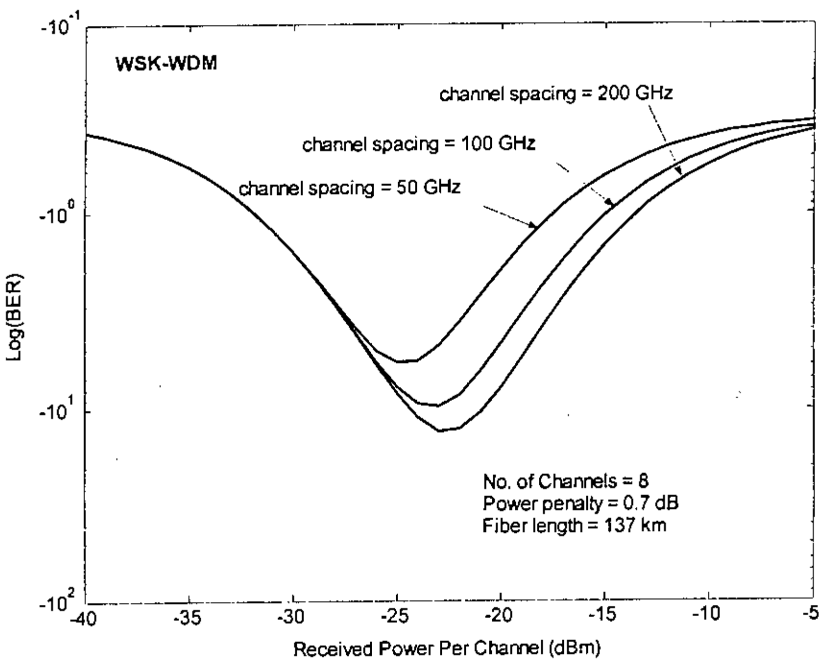

Fig. 5.5: BER versus Received power per channel for different channel spacing

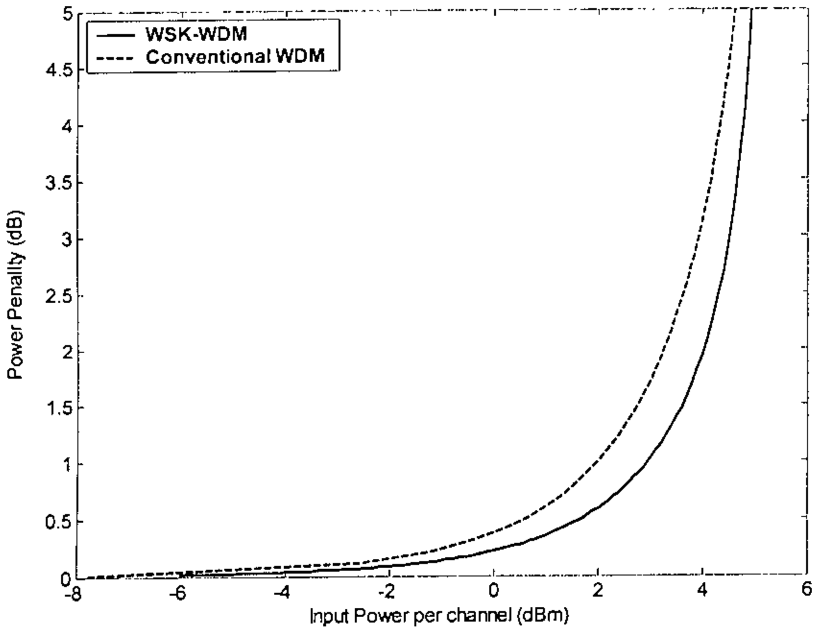

Fig. 5.6: Power penalty as a function of transmitting power for both systems

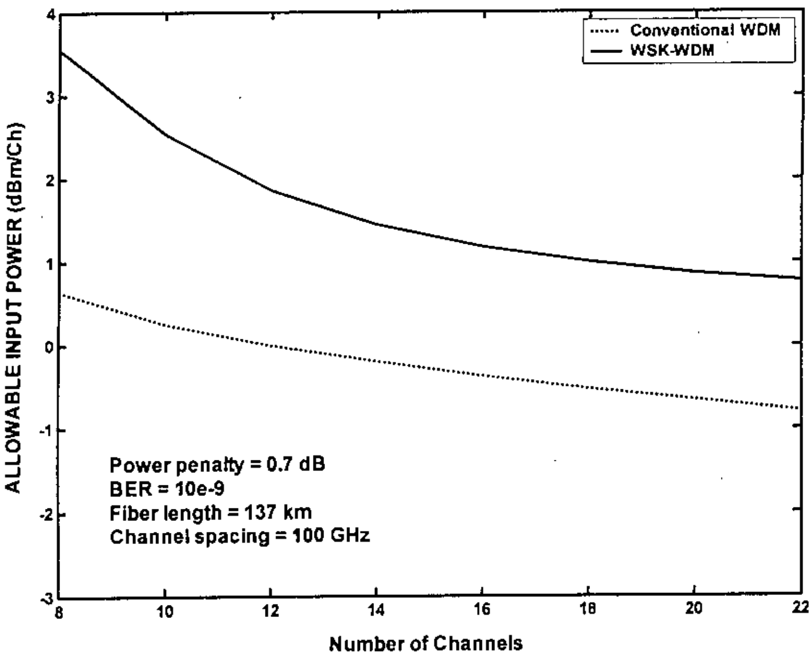

Fig. 5.7: Allowable input power for different number of channels considering the same total bandwidth for both systems

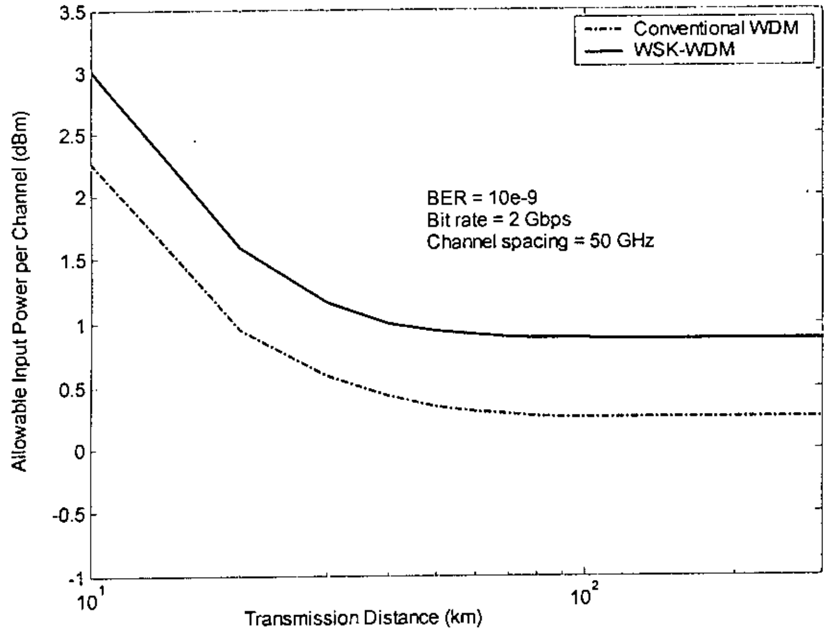

Fig. 5.8: Allowable input power as a function of transmission distance limiting the both systems to the same total bandwidth

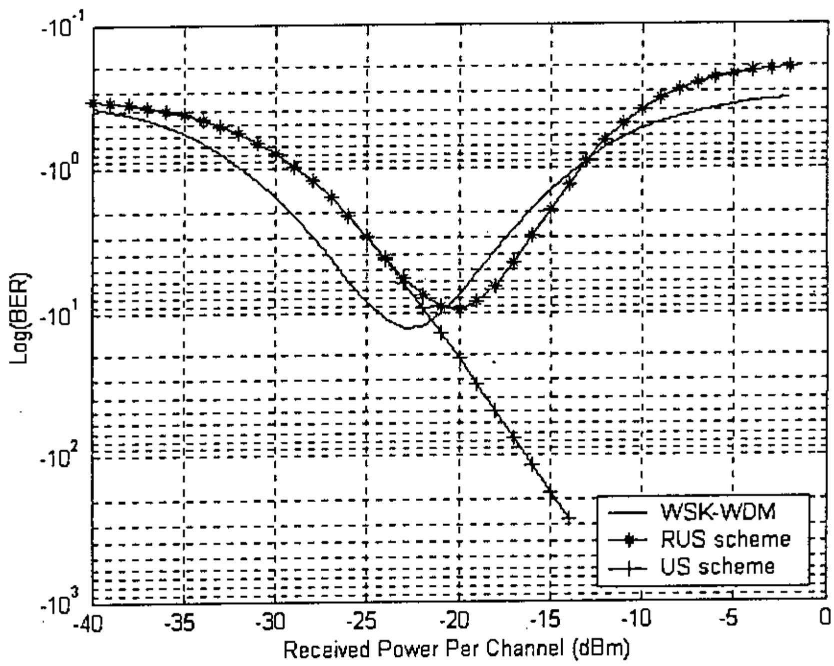

Fig. 5.9: BER comparison among US scheme, RUS scheme and WSK-WDM system employing DSF supporting 8 users

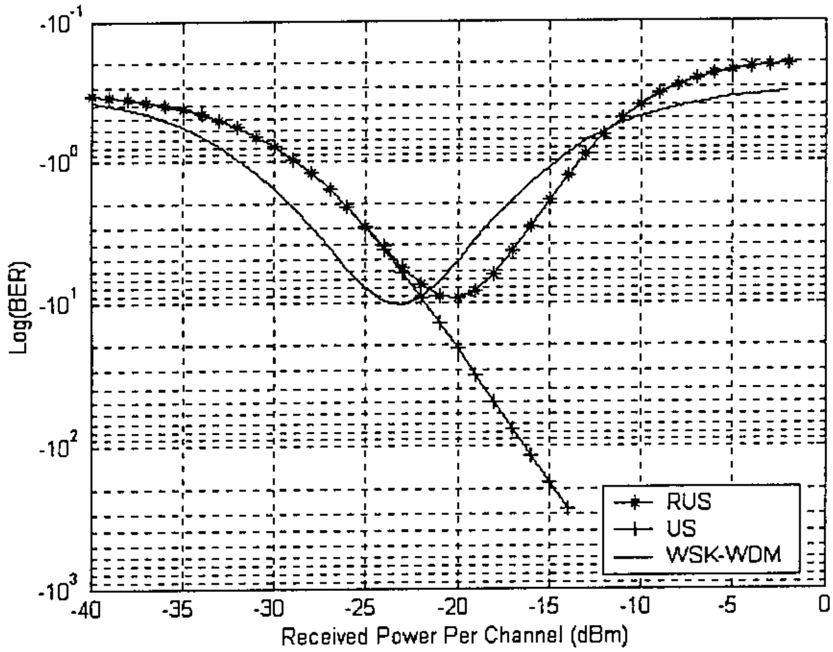

Fig. 5.10: BER comparison among US scheme, RUS scheme and WSK-WDM system employing DSF supporting 10 users

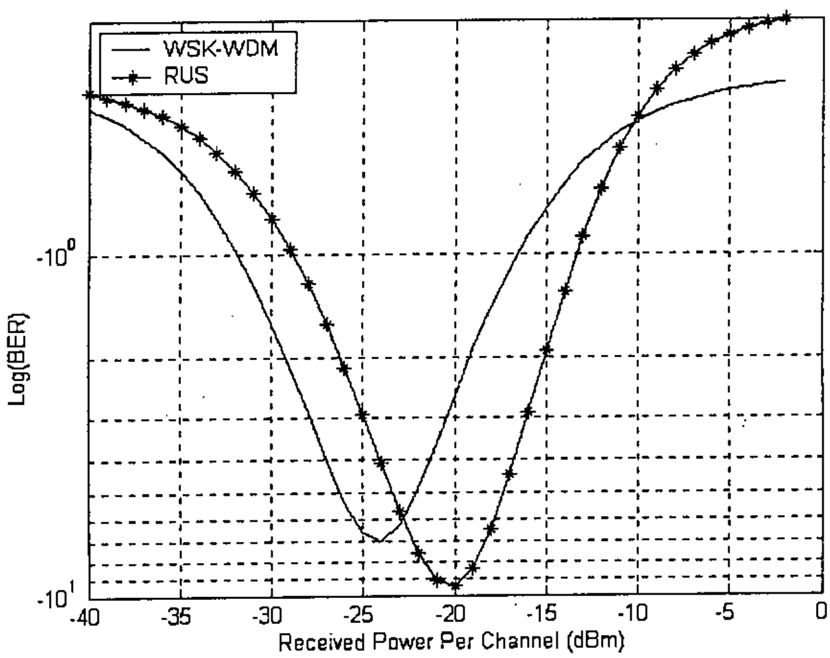

Fig. 5.11: BER comparison between RUS scheme and WSK-WDM system employing DSF supporting 10 users and limiting both systems to the same total bandwidth

5.4 Limitations of Different FWM Reduction Schemes

Limitations of US scheme:

(i) The main problem of US channel allocation technique is the expansion of total bandwidth with the increase of number of users. This scheme requires much wider bandwidth compared to equal channel spacing scheme. The optimized total bandwidth of US system is given by [16]

$$B_{un} = \left(1 + \frac{N/2 - 1}{n}\right) B_{eq} \tag{5.1}$$

where $B_{eq} = (N-1)\Delta f_c$ is total optical bandwidth of a conventional WDM system with the channels equally spaced by Δf_c.

(ii) In US scheme, it can be ensured that no FWM product terms will fall on to any signal frequencies by appropriate unequal channel spacing. But the newly generated FWM products can mix with channel frequencies or themselves to produce higher-order FWM products, which can overlap with existing channels and result in FWM crosstalk [39].

(iii) Although the FWM lights do not coherently interfere with the signals, the FWM waves are still generated at the expense of the transmitted power, giving rise to pattern-dependent depletion of the channels. The system performance is limited by the channel power depletion and it may cause serious performance degradation especially when the signal power level is high or number of users is large.

Limitations of RUS scheme:

(i) RUS channel allocation technique gives much better performance than equally spaced conventional WDM system, but the performance is somewhat worse than US scheme. Because, there are some FWM products interfering with the signal frequencies.

(ii) Like US scheme, channel power depletion causes serious performance deterioration when power density and number of channels are high.

(iii) Higher-order FWM products also impair the system performance.

Limitations of WSK-WDM scheme:

(i) The total optical bandwidth increases linearly with number of channels.

(ii) Channel power depletion degrades the system performance.

(iii) Higher-order FWM crosstalks also deteriorate the performance.

5.5 Evaluation of Power Depletion for Equally Spaced Channels

Signal power depletion due to FWM process is unavoidable for both equal and unequal channel spacing systems in case of sufficiently large input powers. Consider three copropagating channels with powers P_1, P_2 and P_3, and if the energy is coupled from P_1 to P_2 and P_3, the solutions of coupled-mode equations can be written as [40]

$$Q_1 = P_1(0)y$$
$$Q_2 = 0.5P_1(0)(1-y)+P_2(0)$$
$$Q_3 = 0.5P_1(0)(1-y)+P_3(0) \tag{5.2}$$

where y is a function of z to be determined. For the initial condition of $P_3(0)=0$ which corresponds to the cases of maximum energy coupling y is given by

$$y=\frac{r+1}{r\cosh^2(\sqrt{r+1}f+1)} \tag{5.3}$$

where $r \equiv 2P_2(0)/P_1(0)$ and $f = \gamma P_1(0)[1-\exp(-\alpha z)]/\alpha$, here γ is the nonlinearity coefficient of fiber. For multichannel communication systems, $P_3(0)$ cannot be ignored and for this case y is given as

$$y = \frac{4\bar{r}^{-2}\exp(2\bar{r}f)}{r_0^2\exp(4\bar{r}f) + 2(2+r_2+r_3)\exp(2\bar{r}f)} + r_0^{-2}(r_3-r_2)^2 \tag{5.4}$$

with

$r_2 = 2P_2(0)/P_1(0)$

$r_3 = 2P_3(0)/P_1(0)$

$\bar{r} = \sqrt{(1+r_2)(1+r_3)}$

$r_0 = \sqrt{r_3(r_2+1)} + \sqrt{r_2(r_3+1)}$

Depending on the relative phase of the three waves, either P_1 is a decreasing function of z i.e. energy is transferred from P_1 to P_2 and P_3, or energy is transferred from P_2 and P_3 to P_1. The power depletion of the channel can be determined by solving the above equations. The above equations can be used for both equally spaced and unequally spaced channels. It has been found that signal power depletion in equal channel spacing system is more severe compared to unequal channel spacing system.

5.6 Evaluation of Power Depletion for Unequally Spaced Channels

For intensity-modulated repeaterless WDM systems with unequal channel spacings, a more accurate expression for channel power depletion due to generation of FWM waves considering nondegenerate case only, which is the worst one, can be deduced as [38]

$$D_k = \tanh^2(KP\sqrt{kL_{eff}}) \qquad k \in (0, 1\ldots, N\text{-}2) \tag{5.5}$$

with probability

$$P_D(k) = \binom{N-2}{k}\left(\frac{1}{2}\right)^{(N-2)} \tag{5.6}$$

where $K = \dfrac{32\pi^3}{n^2 \lambda c A_{eff}} D\ \chi_{1111}$ and maximum depletion can be computed as

$$D_M = \tanh^2(KP\sqrt{(N-2)L_{eff}}) \tag{5.7}$$

The probability of error for a particular channel m is given by

$$P_e = \frac{1}{2}P_{e|0}(I_{th}) + \frac{1}{4}P_{e|1,0}(I_{th}) + \frac{1}{4}\sum_D P_{e|1,1,D}(I_{th})P_D \tag{5.8}$$

where I_{th} is the threshold level of the decision circuit at the receiver, $P_{e|0}$ is the probability of error when a "0" is transmitted, $P_{e|1,0}$ is the probability of error when a "1" has been transmitted on m channel and a "0" on channel m+1, and $P_{e|1,1,D}$ is the probability of error when a "1" has been transmitted both on channel m and on channel m+1.

5.7 Conclusion

In this chapter, the performance of WSK-WDM system is investigated and demonstrated theoretically. The system performance of WSK-WDM is compared to that of conventional on-off WDM and also to other FWM reduction schemes. Both conventional WDM and WSK-WDM systems employ equal channel spacing, which is simple and can be easily upgraded or modified, whereas US and RUS schemes use unequally spaced channel allocation technique, which is complex. If we compare WSK-WDM with RUS channel allocation technique, it may be concluded that WSK-WDM is a simpler scheme and can provide improved performance than RUS scheme, but it requires more bandwidth to support the same number users. In addition to this, WSK-WDM is more noise resistant.

Chapter 6
FWM REDUCTION BY A COMBINATION OF WSK TECHNIQUE AND DISPERSION MANAGEMENT

6.1 Introduction

Conventional WDM or WSK-WDM system assumes uniform dispersion throughout the entire length and employ low dispersion fibers to keep minimum chromatic dispersion. Consequently, these systems suffer performance degradation due to FWM effect. Although US scheme, RUS scheme or WSK technique improve the system performance, there is still some effect, such as, channel power depletion or interference that may impair the performance severely at large power levels. A combination of unequal channel spacing or repeated unequal channel spacing with dispersion compensation has been examined and shown that the overall performance is much improved [18]. In this chapter, a combination of WSK technique with dispersion management will be investigated and the performance attained will be compared to that of other systems already discussed in the previous chapters.

6.2 FWM Reduction by Dispersion Management

Phase matching among the copropagating channels is one of the conditions for occurrence of sufficient FWM effect. In case of zero or low dispersion fibers, phase matching is created as the difference in group velocity among different signals is low. So by keeping high chromatic dispersion, effect of FWM can be reduced. But high chromatic dispersion causes pulse broadening as group velocity of copropagating signals increases, thereby creating inter symbol interference (ISI) and ultimately degrades the system performance. Even when the nonlinear effects are not important, dispersion-induced pulse broadening can be detrimental for optical fiber communication systems. Therefore, this problem can be solved by using different types of fibers with different chromatic dispersions for the transmission span. One type of fibers will have a positive chromatic dispersion, while other type will have negative dispersion such that overall dispersion for the entire transmission length will be minimum to ensure that system performance is not degraded much.

System Description: Consider an actual WDM transmission system in which the transmission line is composed of short lengths of fiber with different zero dispersion wavelengths. The general expression for FWM power generated in a WDM system with nonuniform chromatic dispersion is given as [41]

$$P_{FWM} = \frac{1024\pi^6}{n_o^4 \lambda^2 c^2} (D\chi)^2 \frac{P_p P_q P_r}{A_{eff}^2} e^{-\alpha L} \left| \sum_{m=1}^{M} \exp\left[i \sum_{k=1}^{m-1} \Delta\phi^{(k)} \right] \times \sum_{n=1}^{N} \exp\left[\sum_{j=1}^{n-1} \left(-\alpha + i\Delta\beta^{mj}\right) L_0 \right] \times \frac{1 - \exp\left[\left(-\alpha + i\Delta\beta^{mn}\right) L_0\right]}{\alpha - i\Delta\beta^{mn}} \right|^2 \tag{6.1}$$

where A_{eff} is effective mode area in core, P_p, P_q and P_r are the input powers of channels p, q and r respectively, D is the degeneracy factor, L_0 is the length of one fiber, N is number of fiber in one section, $L = NL_0$ is the length of one section, α is the attenuation loss coefficient, $\Delta\beta^{mn}$ is the phase mismatch in fiber n of mth section and be given by

$$\Delta\beta^{mn} = \beta_p^{(mn)} + \beta_q^{(mn)} - \beta_r^{(mn)} - \beta_F^{(mn)} \tag{6.2}$$

and $\Delta\phi^{(k)}$ is the propagation phase difference of lights p, q, r in section k, and can be written as

$$\Delta\phi^{(k)} = \phi_p^{(k)} + \phi_q^{(k)} - \phi_r^{(k)} - \phi_F^{(k)} \tag{6.3}$$

Now, dispersion compensation may be incorporated to the existing WDM transmission system. A highly dispersive fiber with positive dispersion coefficient is used in each section so that at the end of the fiber lights are highly phase mismatched and the FWM effect is reasonably reduced, to compensate this high value of dispersion, another fiber with opposite polarity dispersion i.e. low dispersive fiber with negative dispersion coefficient is used in cascade so that overall dispersion remains minimum.

There are three different types of dispersion management schemes [42], which are briefly characterized below:

(i) Dispersion Shifted Fiber and Dispersion Shifted Fiber (DSF + DSF): In this dispersion management scheme, two types of dispersion shifted fiber are incorporated by using equal length of each fiber DSF_1 and DSF_2. For a particular wavelength the fibers are arranged so that the dispersion values alternate between them, say +2.5 ps/nm-km and –2.5 ps/nm-km. This type of fibers is termed as Non-Zero dispersion shifted fiber (NZDSF).

(ii) Dispersion Shifted Fiber and Conventional Fiber (DSF + SMF): In that case the link is composed of dispersion shifted fiber with negative dispersion coefficient and conventional single-mode fiber with positive dispersion. As for example, the fibers are arranged such that dispersions alternate between –2.5 ps/nm-km and +17.5 ps/nm-km with different fiber lengths.

(iii) Conventional Fiber and Dispersion-Compensating Fiber (SMF + DCF): In this scheme convention single-mode fiber with positive dispersion and dispersion-compensating fiber with large negative dispersion are used. The fibers are arranged such that fiber length of each type is different and the dispersions alternate between +17 ps/nm-km and –85 ps/nm-km.

In our model we will employ two fibers in a section of length L_0 i.e. fiber length of mth section $L_0^{(m)}$ is composed of two different fibers characterized by attenuation $\alpha_{1,2}$, dispersion coefficient $D_{c1,2}$, dispersion slope $dD_{c1,2}/d\lambda$ and length $L_0^{m1,2}$, such that

$L_0^{(m)} = L_0^{(m1)} + L_0^{(m2)}$ and $D_{c1}L_0^{(m1)} + D_{c2}L_0^{(m2)} = 0$ or $D_{c1}L_0^{(m1)} = -D_{c2}L_0^{(m2)}$. We will adjust the dispersion and length such that the overall dispersion of the total transmission length becomes minimum. The phase mismatch for this case is

$$\Delta\beta^{mn} = \beta_p^{(mn)} + \beta_q^{(mn)} - \beta_r^{(mn)} - \beta_F^{(mn)}$$

$$= (f_p - f_r)(f_q - f_r)\frac{2\pi\lambda^2}{c}\left[D_{c1,2}(\lambda) - \{(f_p - f_0^{mn}) + (f_q - f_0^{mn})\}\frac{\lambda^2}{2c}\frac{dD_{c1,2}(\lambda)}{d\lambda}\right] \tag{6.4}$$

where $D_{c1,2}$ is dispersion coefficient of fiber 1 (D_{c1}) and 2 (D_{c2}) and f_0^{mn} is zero-dispersion frequency of fiber n in section m. The expression for FWM power for this model is

$$P_{FWM} = \frac{1024\pi^6}{n_o^4\lambda^2c^2}(D\chi)^2\frac{P_pP_qP_r}{A_{eff}^2}e^{-(\alpha_1L_0^1+\alpha_2L_0^2)}\left|\sum_{m=1}^{M}\exp\left[i\sum_{k=1}^{m-1}\Delta\phi^{(k)}\right]\times\sum_{n=1}^{N}\exp\left[\sum_{j=1}^{n-1}\left(-\alpha_{1,2}^{mj}+i\Delta\beta^{mj}\right)L_0^{mj}\right]\times\frac{1-\exp\left[\left(-\alpha_{1,2}^{mn}+i\Delta\beta^{mn}\right)L_0^{mn}\right]}{\alpha_{1,2}^{mn}-i\Delta\beta^{mn}}\right|^2 \tag{6.5}$$

The expression for received power is

$$P_r = L_rPe^{-(\alpha_1L_0^1+\alpha_2L_0^2)\times m} \tag{6.6}$$

6.3 Impact Of Chromatic Dispersion

In this subsection we will present the effect of chromatic dispersion on the system performance. From the above discussion it is obvious that FWM generation efficiency decreases with the increase of fiber chromatic dispersion, which is illustrated in Figure 6.1. The BER performance of the WSK-WDM system shows a significant improvement due to use of dispersive fiber, which is depicted in Figure 6.2. Similarly higher chromatic dispersion also improves the performance of allowable input power, i.e., the maximum transmitting power restricted by accumulation of FWM power will be increased, because FWM generation is reduced by dispersion. Figure 6.3 indicates the validity of this argument.

From above discussion and analysis, it is clear that dispersive fibers are better than low dispersion fibers, since they reduce FWM effect and thereby enhance the system performance. But, on the other hand, chromatic dispersion produces pulse broadening, i.e., ISI which ultimately badly impairs the performance. So, we must apply some compensation mechanism to keep overall dispersion as minimum as possible.

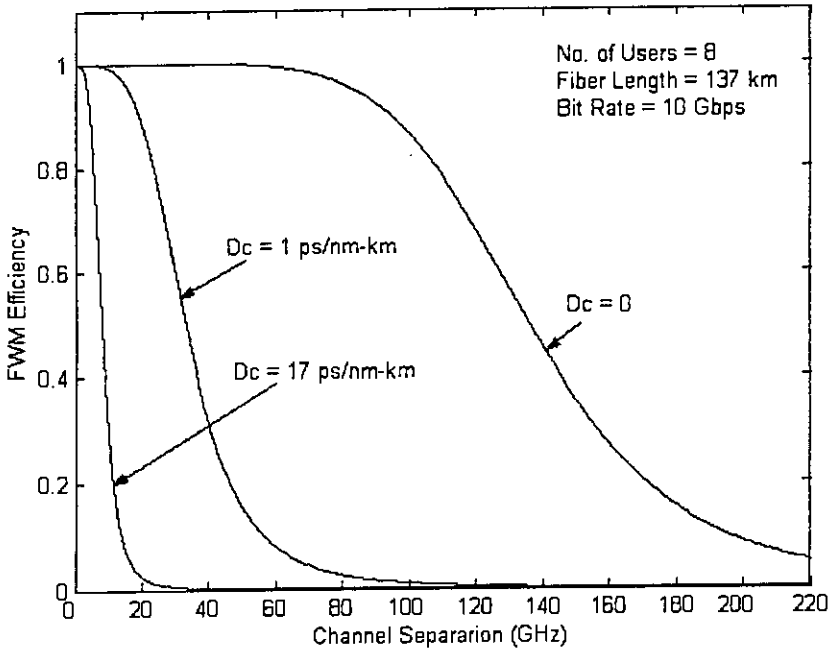

Figure 6.1: FWM generation efficiency (η) versus channel separation for different chromatic dispersion.

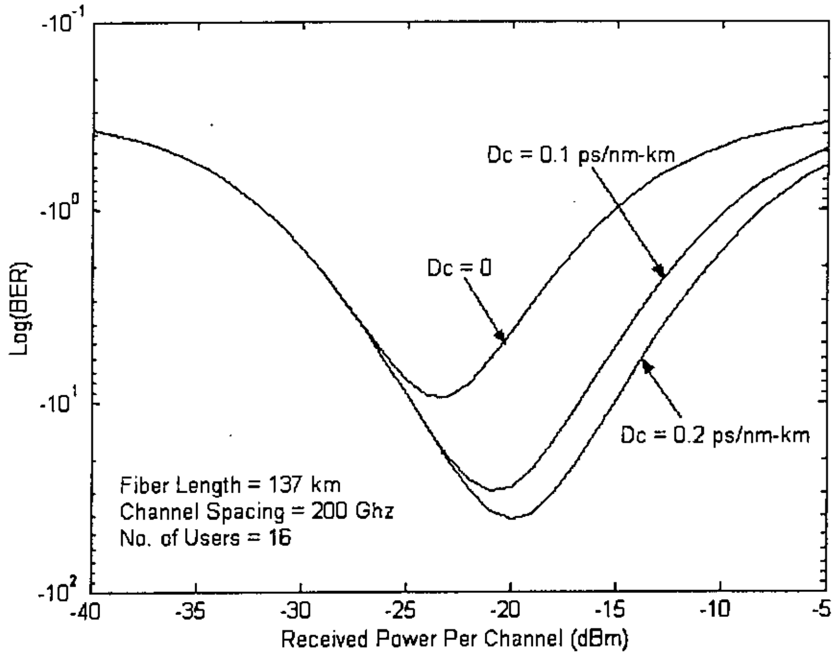

Figure 6.2: BER of WSK-WDM system for different chromatic dispersion supporting 16 users.

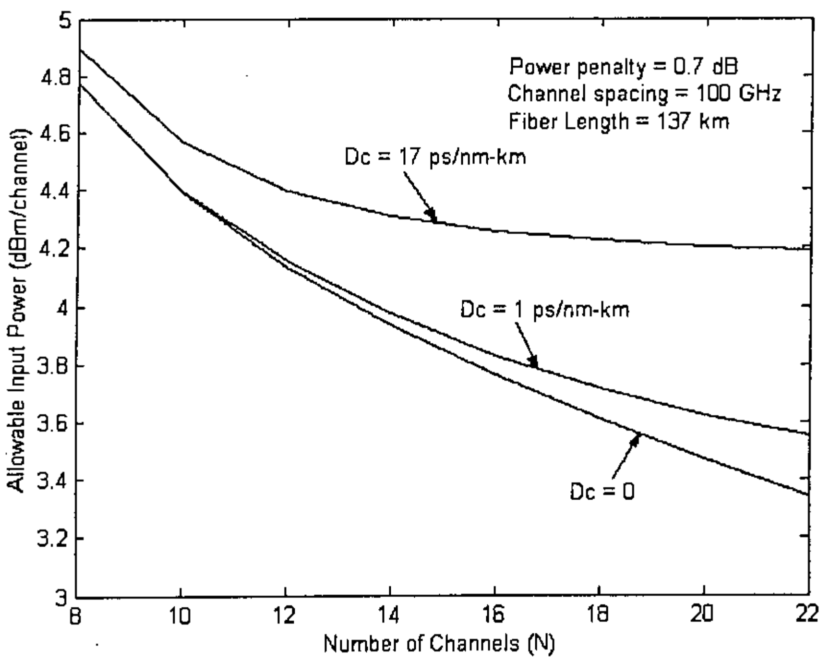

Figure 6.3: Allowable input power per channel versus number channels for different chromatic dispersion of WSK-WDM system.

6.4 WSK-WDM System with Dispersion Management Scheme

The performance of WSK-WDM system is analyzed employing dispersion management scheme using the system parameters described in the previous chapters. Using the model described above, each section of the transmission line is composed of two different fibers. We will consider two types of dispersion compensation schemes like (DSF + DSF) and (DSF + SMF) that are already defined.

WSK-WDM system with (DSF + DSF) scheme (Combined-1): This combined system consists of 4 sections, each of which has two dispersion-shifted fibers DSF_1 and DSF_2,

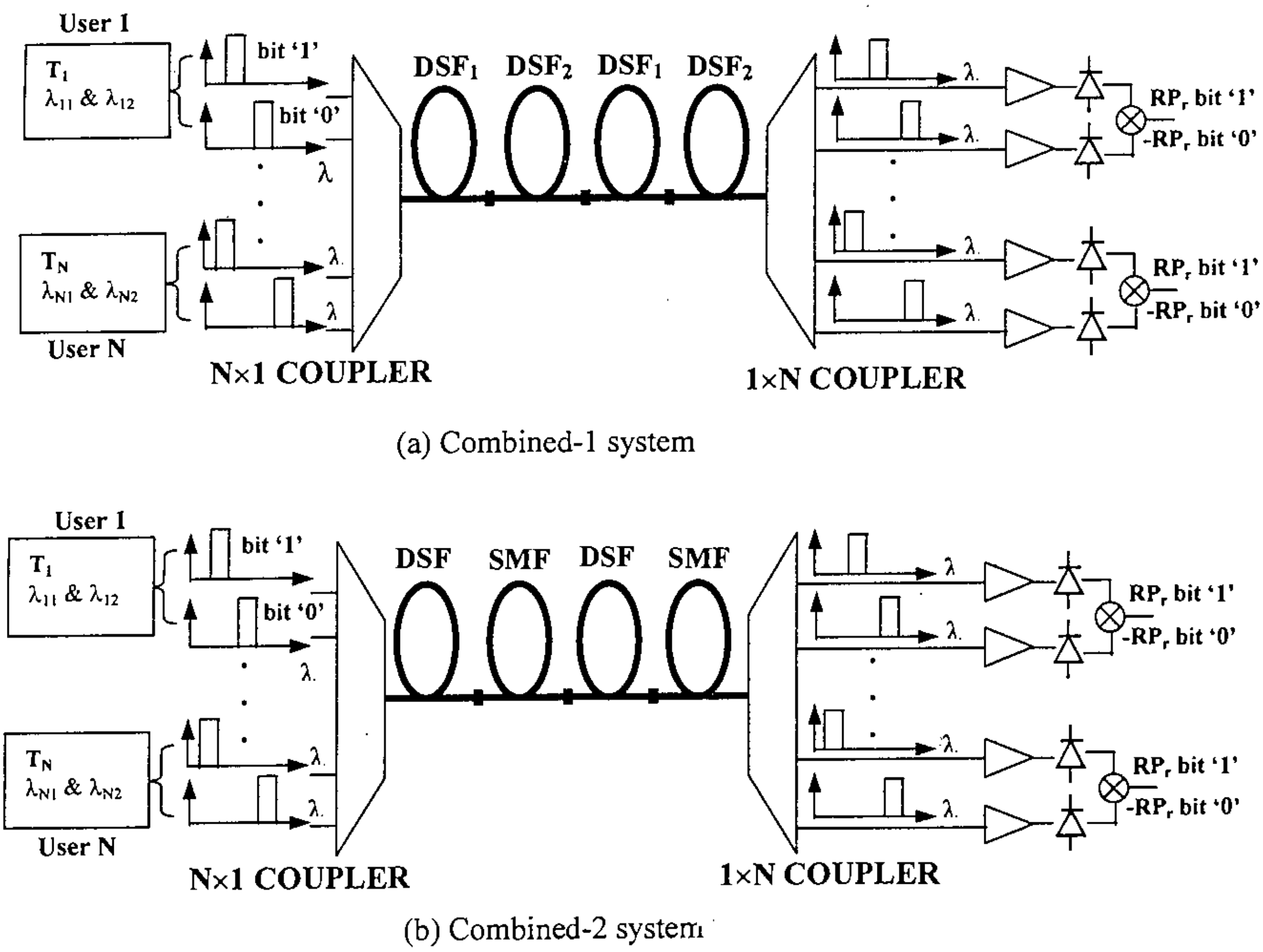

(a) Combined-1 system

(b) Combined-2 system

Figure 6.4: Schematic block diagrams of the Combined systems

with equal length and equal dispersion but have opposite polarity. DSF_1 has dispersion value of +2.5 ps/nm-km and DSF_2 has –2.5 ps/nm-km, and each of the fiber is 17.125 km long. The total fiber length is 137 km.

WSK-WDM system with (DSF + SMF) scheme (Combined-2): This combined system has 3 sections, each consists of two different fibers, one is dispersion shifted fiber (DSF) with dispersion of –2.4 ps/nm-km and length 40 km and the other is conventional single mode fiber (SMF) with dispersion 17 ps/nm-km and length 5.667 km. The total length of fiber is 137 km.

Table-4: Fiber and system parameters used in the Combined systems

No. of Users	8
Fiber length	137 km
Channel spacing	200 GHz
Bit Rate	10 Gbps
Dispersion (DSF)	0 ps/nm-km
Dispersion (NZDSF)	-2.4 ps/nm-km
Dispersion (SMF)	17 ps/nm-km
Dispersion slope (DSF)	0.055 ps/nm^2-km
Dispersion slope (NZDSF)	0.07 ps/nm^2-km
Dispersion slope (SMF)	0.09 ps/nm^2-km

6.5 Results

The performance of combined systems, WSK-WDM with (DSF + DSF) scheme denoted as Combined-1 and WSK-WDM with (DSF + SMF) scheme denoted as Combined-2, are investigated and compared to that of previous system employing uniform dispersion.

6.5.1 Bit Error Rate

Figure 6.5 shows the BER curves for different systems under consideration. It can be observed that WSK-WDM system provides better performance than conventional on-off WDM system; and WSK-WDM system with dispersion management scheme gives much better performance than WSK-WDM using uniform dispersion. Minimum BER achievable from WSK-WDM system is 10^{-13}, whereas it is lower than 10^{-73} in Combined-1 scheme and lower than 10^{-193} in Combined-2 system. The combined systems offer much improved performance by reducing FWM effect; at the same time they maintain low overall chromatic dispersion as well.

6.5.2 Power Penalty

The power penalty suffered by the systems to attain a BER of 10^{-9} is assessed and is illustrated in Figure 6.6. The combined systems provide much better results with respect to WSK-WDM using uniform dispersion.

6.5.3 Allowable Input Power

For a given power penalty of 0.7 dB at a BER of 10^{-9} the maximum allowable input power is found to be restricted by FWM powers. The FWM power increases as P^3. At high transmitting power, FWM causes a serious limitation on system performance. Allowable input power per channel for various schemes is evaluated and plotted as a function of number of channels, which is shown in Figure 6.7. And allowable transmitting power per channel is also calculated and plotted against transmission lengths, which is illustrated in Figure 6.8. It's clear that the combined systems permit much higher allowable input power to attain a given BER and thus yield much enhanced results.

6.5.4 Bit Rate-Distance Product

Allowable input power is calculated for various transmission distances to achieve a BER of 10^{-9} and the bit rate of 10 Gbps limiting all systems to the same total bandwidth, which is illustrated in Figure 6.8. It shows that for a given BER of 10^{-9}, the combined systems allow longer repeater spacing than WSK-WDM system for the same number of users.

Using the parameters mentioned in Table 5, the overall capacity is predicted to be 10.752 THz-km for WSK-WDM system at the bit rate of 2 Gbps, for Combined-1 system it is 11.136 THz-km, and for Combined-2 system it is 11.968 THz-km. For the bit rate of 10 Gbps, the overall capacities of conventional WDM, WSK_WDM, Combined-1 and Combined-2 systems are 16.8, 36.48, 40 and 44.8 THz-km respectively. The comparison is done considering that each system occupies the same total bandwidth. The combined systems allow longer repeater spacing and enhanced overall system capacity.

Table-5: System parameters and Bit rate-distance comparison including the Combined systems

Parameters	Conventional WDM		WSK-WDM		Combined-1		Combined-2	
BER	10^{-9}		10^{-9}		10^{-9}		10^{-9}	
Channel spacing	100 GHz		50 GHz		50 GHz		50 GHz	
No. of users	16		16		16		16	
Bit Rate	2 Gbps	10 Gbps	2 Gbps	10 Gbps	2 Gbps	10 Gbps	2 Gbps	10 Gbps
Maximum repeater span	155 km	105 km	168 km	114 km	174 km	125 km	187 km	140 km
Bit rate ×Distance	4.96 THz-km	16.8 THz-km	10.752 THz-km	36.48 THz-km	11.136 THz-km	40 THz-km	11.968 Thz-km	44.8 THz-km

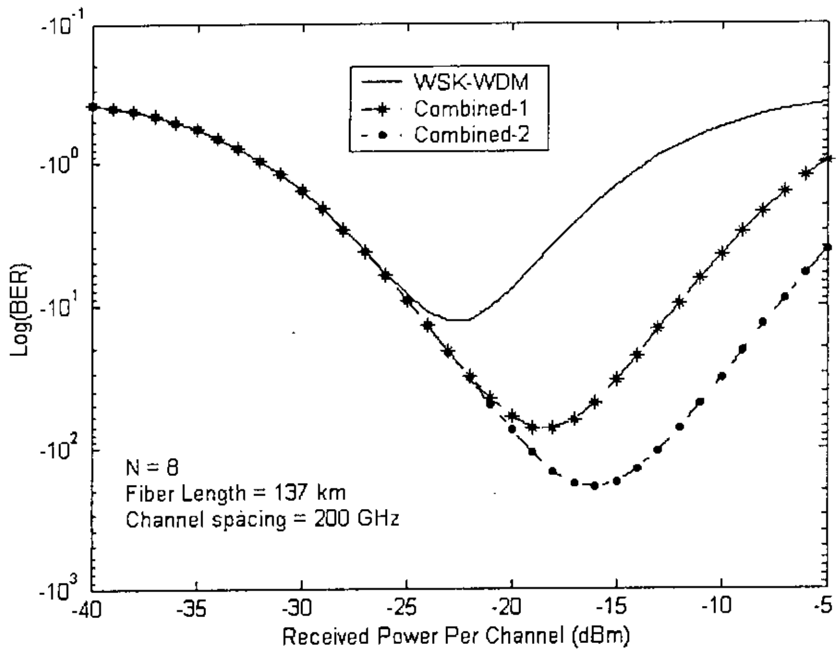

Figure 6.5: Error probability of various schemes as a function signal power

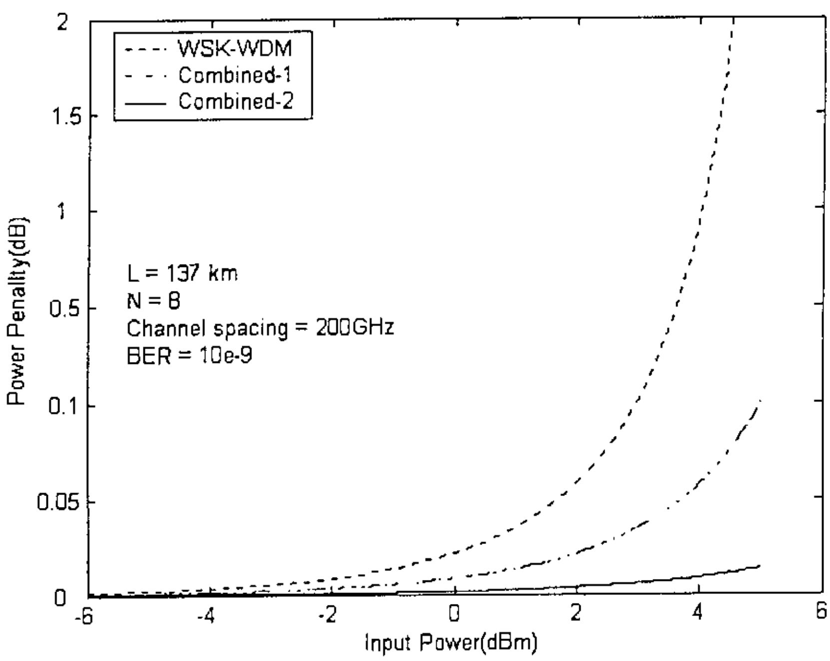

Figure 6.6: Power penalty versus transmitting power per channel for various systems

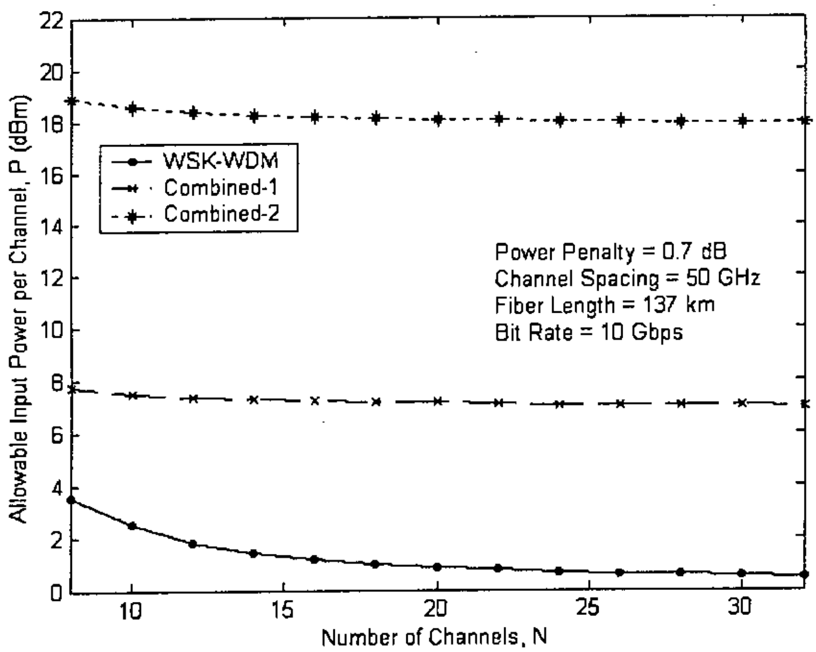

Figure 6.7: Allowable input power versus number of channels for various systems limiting to the same total bandwidth.

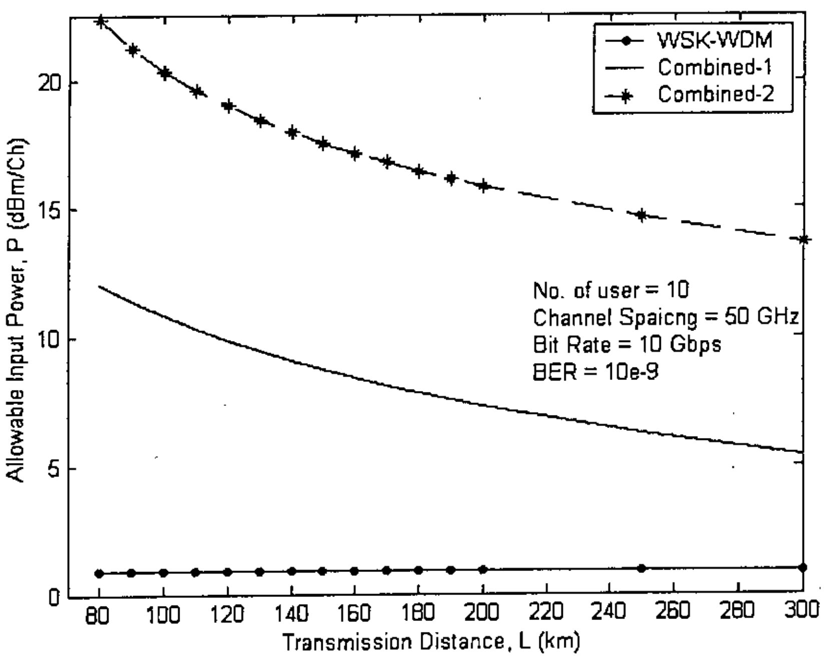

Figure 6.8: Allowable input power per channel as a function of transmission distance for various systems.

6.6 Conclusion

In this chapter the performance of WSK-WDM system with different dispersion management schemes have been analyzed and compared to that of other systems already discussed. The effect of chromatic dispersion on the system performance is investigated and observed that the performance can be improved by adding dispersive fibers but at the same time the overall dispersion must be kept minimum to avoid ISI. Therefore, the combined systems that are the combination of WSK-WDM and dispersion compensation schemes have the overall performance which is much improved from the other systems. Although the combined systems incur some complexity, substantial improvement can be achieved in the system performance, such as, power penalty, allowable input power and bit rate-distance product, which are much more for a given BER than that of conventional WDM or WSK-WDM.

Chapter 7
CONCLUSION

7.1 Conclusion of this Study

A rigorous analysis has been carried out to evaluate the performance of WSK-WDM system in presence of four-wave mixing (FWM). The WSK-WDM system exhibits promising features that will be useful for future high speed, long distance optical networks. The commercial lightwave communication networks use low dispersion fibers to provide gigabit services by keeping dispersion effect as minimum as possible. FWM then becomes the major source of nonlinear effects causing interchannel crosstalk and channel power depletion and thereby degrading the system performance. It has been observed that the performance of conventional on-off WDM system employing low dispersion fibers is not satisfactory; rather the performance is further deteriorated when number of channels is large or input power per channel is high. WSK-WDM system can provide better performance by depressing the FWM crosstalk. The performance of WSK-WDM system is also compared to that of unequally spaced channel (US) scheme and repeated unequal channel spacing (RUS) scheme. US scheme is the best but at the cost of huge bandwidth. In between WSK technique and RUS scheme, the former is better but it requires relatively large bandwidth for the same number of users; when both systems are analyzed limiting to the same total bandwidth for the same number of users, RUS scheme gives better performance. A remarkable improvement in system performance can be achieved by utilizing the combined systems, which are combinations of wavelength shift keying technique and dispersion management schemes in optical WDM systems. These combined systems offer much better performance; they give much lower bit error rate (BER), larger bit rate-distance product within one repeaterless span and allow narrower channel spacing. Maximum allowable input power per channel is much higher than that of other systems. The balanced configuration of the receiver yields 3dB sensitivity and also cancels other noise that have symmetric spectrum. Therefore, these schemes will also be attractive for DWDM networks.

7.2 Suggestion for Future Works

In our work we have assumed that the fibers used in the transmission system are perfect; actually the zero dispersion wavelength may shift around a small amount along the fiber. Therefore, a study on how WSK-WDM system performs under this imperfect condition is of interest. In the calculation of bit error rate (BER), we have not encountered the response of the optical filters and amplifier noise, and if fiber amplifiers are used, then FWM effect in these fibers will also have to be taken into account. Moreover, we have analyzed the systems considering only a repeaterless network. So there is an opportunity to analyze the multi-channel multi-repeater systems (WSK-WDM and the Combined systems) considering amplifier noise along with shot noise, thermal noise and FWM noise. Polarization states of all input lights are assumed to be identical; in fact, polarization states of the lights are various i.e. they change randomly when propagating through a fiber line. Polarization mode dispersion is also ignored. Future studies may include other linear and non-linear effects into account to realize a complete picture of the system performance.

BIBLIOGRAPHY

[1] M. S. Borella, J. P. Jue, D. Banerjee, B. Ramamurthy, and B. Mukherjee, "Optical components for WDM lightwave networks," *Proc. IEEE*, vol. 85, no. 8, 1997.

[2] J. M. Senior, *Optical Fiber Communications*, 2nd Ed., New Delhi: Prentice-Hall of India, 2002.

[3] P. S. Henry, "Lightwave primer," *IEEE J. Quantum Electron.*, vol. QE-21, no. 12, 1985.

[4] J. Gower, *Optical Communication Systems*, 2nd Ed., New Delhi: Prentice-Hall of India, 2001.

[5] H. Toba, K. Oda, K. Nakanishi, N. Shibata, K. Nosu, N. Takato, and M. Fukuda, "A 100-Channel optical FDM transmission/distribution at 622 Mb/s over 50 km," *IEEE J. Lightwave Technol.*, vol. 8, no. 9, pp. 1396-1401, 1990.

[6] A. R. Chraplyvy, "Limitations on lightwave communications imposed by optical nonlinearities," *J. Lightwave Technol.*, vol. 8, no. 10, pp. 1548-1557, 1990.

[7] F. Forghieri, R. W. Tkach, A. R. Chraplyvy, A. H. Gnauck, R. M. Derosier, "Four-photon mixing and high speed WDM systems," *IEEE J. Lightwave Technol.*, vol. 13, no. 5, pp. 841-849, 1995.

[8] N. Shibata *et al.*, "Crosstalk due to three-wave mixing in a coherent single-mode transmission line," *Electron. Lett.*, vol. 22, p. 675, 1986.

[9] K. Inoue and H. Toba, "Error-rate degradation due to fiber four-wave mixing in four-channel FSK direct-detection transmission," *IEEE Photon. Technol. Lett.*, vol. 3, no. 1, pp. 77-79, 1991.

[10] R. G. Waarts and R. P. Braun, "System limitations due to four-wave mixing in single mode optical fibers," *Electron. Lett.*, vol. 22, no. 16, pp. 873-875, 1986.

[11] M. W. Maeda, W. B. Seesa, W. I. Way, A. Yi-Yan, L. Curtis, R. Spicer, and R. I. Laming, "The effect of four-wave mixing in fibers on optical frequency-division multiplexed systems," *IEEE J. Lightwave Technol.*, vol. 8, no. 9, pp. 1402-1408, 1990.

[12] N. Shibata, R. P. Braun, and R. G. Waarts, "Phase-mismatch dependence of efficiency of wave generation through four-wave mixing in a single-mode optical fiber,"

IEEE J. Quantum Electron., vol. QE-23, no. 7, pp. 1205-1210, 1987.

[13] R. H. Stolen, "Parametric amplification and frequency conversion in optical fibers," *IEEE J. Quantum Electron.*, vol. QE-18, pp. 1062-1072, 1982.

[14] K. O. Hill, D. C. Johnson, B. S. Kawasaki and R. I. Macdonald, "CW three wave mixing in single mode optical fibers," *J. Appl. Phys.*, vol. 49, pp. 5098-5106, 1978.

[15] N. Henmi, Y. Aoki, T. Ogata, T. Saito, and S. Nakaya, "A new design arrangement of transmission fiber dispersion for suppressing nonlinear degradation in long-distance optical transmission systems with optical repeater amplifiers," *IEEE J. Lightwave Technol.,* vol. 11, no. 10, pp. 1615-1621, 1993.

[16] F. Forghieri, R. W. Tkach, A. R. Chraplyvy and D. Marcuse, "Reduction of four-wave mixing in WDM systems using unequally spaced channels," *IEEE Photon. Technol. Lett,* vol. 6, no. 6, pp.754-756, 1994.

[17] T. Numai, and O. Kubota, "Analysis of repeated unequally spaced channels for FDM lightwave systems," *IEEE J. Lightwave Technol.,* vol. 18, no. 5, pp. 656-664, 2000.

[18] M. F. Uddin, A. B. M. Nasirud Doulah, A. B. M. Isteak Hossain, M. Z. Alam, and M. N. Islam, "Reduction of four-wave mixing effect in an optical wavelength-division multiplexed system by utilizing different channel spacing and chromatic dispersion schemes," *Opt. Eng.*, vol. 42, no. 9, pp. 2761-2767, 2003.

[19] C. J. Mahon, L. Olofsson, E. Bodtker, and G. Jacobsen, "Polarization allocation schemes for minimizing fiber four-wave mixing crosstalk in Wavelength Division Multiplexed optical communication systems," *IEEE Photon. Technol. Lett.*, vol. 8, no. 4, pp. 575-577, 1996.

[20] DWDM Tutorial (Part II), *Cisco Systems*, Inc., 2000.

[21] *Corning SMF-LS™ CPC6 single-mode non zero dispersion-shifted optical fiber*, Prod. Inform. Sheet PI1050 Corning, NY: Corning Incorporated, Apr. 1997.

[22] Chu Xiang, and James F. Young, "Wavelength shift keying technique to reduce four-wave mixing crosstalk in WDM," *Proc., IEEE LEOS Annual Meeting*, Paper WZ2, pp. 609-610, San Francisco, CA, Nov 1999.

[23] F. Forghieri, R. W. Tkach, A. R. Chraplyvy, "Power limitations due to four-wave mixing depletion in WDM systems with unequally spaced channels," in *Proc. LEOS*

Topical Meeting on "Impact of Fiber Nonlinearities on Lightwave systems", Santa Barbara, CA, paper T1.4, pp. 29-30, July 1993.

[24] G. E. Keiser, *Optical Fiber Technology,* vol. 5, pp. 3-39, 1999.

[25] Akiba, "Optical Submarine Cable Networks," *Proc. IEICE '00,* March 2000.

[26] T. Terahare, T. Hoshida, J. Kumasako, H. Omeka, "128×10.66 Gbits/s transmission over 840 km optical repeater spacing (30.4 dB loss) employing dual-band distributed Raman amplification," *Proc. OFC '00,* Baltimore, March 2000.

[27] G. P. Agrawal, *Nonlinear Fiber Optics*, 2nd Ed., New York: Academic Press, Inc., 1995.

[28] D. Cotter, "Observation of stimulated Brillouin scattering in low-loss silica fiber at 1.3 μm," *Electron. Lett.*, vol. 18, pp. 495-496, 1982.

[29] Application Note 122, © November 2000 by Force, Incorporated. Web page: www.forceinc.com.

[30] R. W. Tkach, A. R. Chraplyvy, and R. M. Derosier, "Impact of parametric gain due to four-photon mixing on lightwave systems," in *Proc. OFC '94*, San Jose, CA, Feb 1994, Paper FC5.

[31] W. C. Babcock, "Intermodulation interference in radio systems," *Bell Syst. Tech. J.*, vol. 31, pp. 63-73, Jan 1953.

[32] K. Inoue, K. Nakanishi, K. Oda, and H. Toba, "Crosstalk and power penalty due to fiber four-wave mixing in multichannel transmission," *IEEE J. Lightwave Technol.*, vol. 12, no. 8, pp. 1423-1439, 1994.

[33] B. Sklar, *Digital Communications,* 2nd Ed., New Delhi: Pearson Education, Inc., 2001.

[34] K. Inoue, H. Toba, and K. Oda, "Influence of fiber four-wave mixing on multichannel FSK direct detection transmission systems," *J. Lightwave Technol.,* vol. 10, no. 3, pp. 350-360, 1992.

[35] F. Foghieri, A. H. Gnauck, R. W. Tkach, A. R. Chraplyvy, and R. M. Derosier, "Repeaterless transmission of eight channels at 10 Gb/s over 137 km (11 Tb/s-km) of dispersion-shifted fiber using unequal channel spacing," *IEEE Photon. Technol. Lett.*, vol. 6, no. 11, pp. 1374-1376, 1994.

[36] M. Faisal, M. N. Islam, and S. P. Majumder, " Performance of Wavelength Shift Keying technique in reducing the four-wave mixing effect in optical WDM system," *Proc. ICEECE '03*, Dhaka, pp. 157-160, December 22-24, 2003.

[37] E. Lichtman, "Bit rate-distance product limitations due to fiber nonlinearities in multichannel coherent optical communication systems," *Electron. Lett.*, vol. 27, no. 9, pp. 757-759, 1991.

[38] F. Forghieri, R. W. Tkach, and A. R. Chraplyvy, "WDM systems with unequally spaced channels," *J. Lightwave Technol.*, vol. 13, no. 5, pp. 889-897, 1995.

[39] S. Song, "Higher-order four-wave mixing and its effect in WDM systems," *Optics Express*, vol. 7, no. 4, pp. 166-170, 2000.

[40] W. Wu, and P. Yeh, "Energy coupling by partially degenerate four-wave mixing in multichannel lightwave systems," *IEEE Photon. Technol. Lett.*, vol. 7, no. 5, pp. 585-587, 1995.

[41] K. Inoue, and H. Toba, "Fiber four-wave mixing in multi-amplifier systems with nonuniform chromatic dispersion," *J. Lightwave Technol.*, vol. 13, no. 1, pp. 88-93, 1995.

[42] X. Y. Zou, M. I. Hayee, S. -M. Hwang, and A. E. Willner, "Limitations in 10 Gb/s WDM optical fiber transmission when using a variety of fiber types to manage dispersion and nonlinearities," *J. Lightwave Technol.*, vol. 14, no. 6, pp. 1144-1152, 1996.

APPENDIX A

Derivation of Expressions for Power Penalty and Allowable Input Power of Conventional WDM System

The signal to noise ratio of a conventional on-off WDM system is given by

$$x = \frac{RP_r - R\left\{\frac{1}{8}\sum_I P_{ijk} + \frac{1}{4}\sum_{II} P_{ijk}\right\}}{\sqrt{N_{FWM} + N_{th} + N_{sh}} + \sqrt{N_{th}}} \tag{A.1}$$

This expression is approximated as (since $RP_r >> R\left\{\frac{1}{8}\sum_I P_{ijk} + \frac{1}{4}\sum_{II} P_{ijk}\right\}$)

$$x = \frac{RP_r}{\sqrt{N_{FWM} + N_{th} + N_{sh}} + \sqrt{N_{th}}} \tag{A.2}$$

We can write the equation as

$$\sqrt{2R^2P_r^2C_{im}^m + N_{th} + N_{sh}} = \frac{RP_r}{x} - \sqrt{N_{th}}$$

$$2R^2P_r^2C_{im}^m + N_{th} + k_sRP_r = \frac{R^2P_r^2}{x^2} + N_{th} - 2\frac{RP_r}{x}\sqrt{N_{th}}$$

$$2RP_rC_{im}^m + k_s = \frac{RP_r}{x^2} - 2\sqrt{N_{th}}/x$$

$$RP_r\left(\frac{1}{x^2} - 2C_{im}^m\right) = k_s + 2\sqrt{N_{th}}/x$$

where C_{im}^m is called the effective FWM crosstalk and is given as

$$C_{im}^m = \frac{1}{8}\sum_I \frac{P_{ijk}}{P_r} + \frac{1}{4}\sum_{II} \frac{P_{ijk}}{P_r} \tag{A.3}$$

N_{FWM}, N_{th} and N_{sh} are FWM noise, thermal noise and shot noise respectively. $N_{sh} = k_s R P_r$ with $k_s = 2qB_e$. R is photodetector's responsivity and P_{ijk} is the FWM power. The summations I and II denote the summation for completely nondegenerate case $i \neq j \neq k$ and partially degenerate case $i = j \neq k$ respectively; P_r is the received power.

The expression for received power to attain a given BER under FWM effect is written as

$$P_r = \frac{1}{R}\left(\frac{k_s + 2\sqrt{N_{th}}/x}{\dfrac{1}{x^2} - 2C_{im}^m}\right) \tag{A.4}$$

The signal power to achieve a given BER without the influence of FWM is obtained from Equation (A.4) with $C_{im}^m = 0$ as

$$P_{r0} = \frac{1}{R}\left(\frac{k_s + 2\sqrt{N_{th}}/x}{\dfrac{1}{x^2}}\right) \tag{A.5}$$

Now using the Equations (A.4) and (A.5), the expression for power penalty at a given value of x_0 is determined as

$$\begin{aligned} P_p &= \frac{P_r}{P_{r0}} \\ &= \frac{1}{1 - 2x_0^2 C_{im}^m} \end{aligned} \tag{A.6}$$

This is the expression for the power penalty of conventional on-off WDM system. This equation can be written as

$$1 - 2x_0^2 C_{im}^m = \frac{1}{P_p}$$

$$1-\frac{1}{P_p}=2x_0^2\left(\frac{P^3}{P_r}C_{im}^{mp}\right)$$

$$P^3=\frac{P\cdot P_r^p}{2x_0^2}\left(1-\frac{1}{P_p}\right)$$

$$P=\left[\left(1-\frac{1}{P_p}\right)\frac{P_r^p}{2x_0^2C_{im}^{mp}}\right]^{\frac{1}{2}} \tag{A.7}$$

where $P_r^p=\frac{P_r}{P}=L_r e^{-\alpha L}$, P is the transmitting power per channel and $C_{im}^{mp}=\frac{P_r}{P^3}C_{im}^{m}$.

This is the expression for allowable input power per channel of a conventional WDM transmission system considering Gaussian approximation.

APPENDIX B

Derivation of Expression for BER of WSK-WDM System

The probability of error of a communication system is given as

$$P_e = Q\left(\frac{\langle S^m \rangle - \langle S^s \rangle}{\sigma_m + \sigma_s}\right) \tag{B.1}$$

where σ_m and σ_s are the square roots of noise power for bit '1's and bit '0's respectively, $\langle S^m \rangle$ and $\langle S^s \rangle$ are the average power for bit '1's and bit '0's respectively; and Q is co-error function and is expressed as

$$Q(x) = \frac{1}{\sqrt{2\pi}} \int_x^{\infty} \exp\left(-\frac{t^2}{2}\right) dt \tag{B.2}$$

where x is signal to noise ratio (SNR) and is given by

$$x = \frac{\langle S^m \rangle - \langle S^s \rangle}{\sigma_m + \sigma_s} \tag{B.3}$$

The values of $\langle S^m \rangle$ and $\langle S^s \rangle$ are obtained from Equation (4.19) and can be written as

$$\langle S^m \rangle = RP_r \quad \text{for 'mark' and} \tag{B.4}$$

$$\langle S^s \rangle = -RP_r \quad \text{for 'space'} \tag{B.5}$$

where R is the responsivity of photodetecter and P_r is the received power.

The decision statistic of this system conforms to antipodal system. The variances of signal power for 'mark' and 'space' can be obtained from Equation (4.21) and be written as

$$\sigma_m^2 = \sigma_F^{(m)2} + N_{th} + N_{sh} \qquad \text{for 'mark'} \tag{B.6}$$

$$\sigma_s^2 = \sigma_F^{(s)2} + N_{th} + N_{sh} \qquad \text{for 'space'} \tag{B.7}$$

where $\sigma_F^{(m)^2}$ and $\sigma_F^{(s)^2}$ are the variances of FWM signal for 'mark' and 'space' respectively, and N_{th} and N_{sh} are the thermal noise and shot noise respectively. Assuming Gaussian distribution for the FWM noise of WSK-WDM system, the variance of this noise is

$$\sigma_F^{(m)2} = 2R^2 P_r \left\{ \frac{1}{8} \sum_I P_{ijk} + \frac{1}{4} \sum_{II} P_{ijk} \right\} \quad \text{for 'mark'} \tag{B.8}$$

and

$$\sigma_F^{(s)2} = 2R^2 P_r \left\{ \frac{1}{8} \sum_I P_{ijk} + \frac{1}{4} \sum_{II} P_{ijk} \right\} \quad \text{for 'space'} \tag{B.9}$$

where P_{ijk} is the four-wave mixing power. Now, assuming all the three noises have Gaussian distribution profile, the SNR is derived applying the Equations from (B.4) to (B.9) to Equation (B.3) as

$$\begin{aligned} x &= \frac{RP_r - (-RP_r)}{\sqrt{\sigma_F^{(m)^2} + N_{th} + N_{sh}} + \sqrt{\sigma_F^{(s)^2} + N_{th} + N_{sh}}} \\ &= \frac{2RP_r}{2\sqrt{\sigma_F^{(m)^2} + N_{th} + N_{sh}}} \\ &= \frac{RP_r}{\sqrt{N_{FWM} + N_{th} + N_{sh}}} \end{aligned} \tag{B.10}$$

where $N_{FWM} = \sigma_F^{(m)^2}$, and we can consider that $\sigma_F^{(m)^2} \approx \sigma_F^{(s)^2}$, assuming perfect fiber with uniform dispersion.

But for exact analysis $\sigma_F^{(m)^2} \neq \sigma_F^{(s)^2}$, since the fibers are not perfect and dispersion is nonuniform; then the SNR becomes

$$\begin{aligned} x &= \frac{RP_r - (-RP_r)}{\sqrt{\sigma_F^{(m)^2} + N_{th} + N_{sh}} + \sqrt{\sigma_F^{(s)^2} + N_{th} + N_{sh}}} \\ &= \frac{2RP_r}{\sqrt{\sigma_F^{(m)^2} + N_{th} + N_{sh}} + \sqrt{\sigma_F^{(s)^2} + N_{th} + N_{sh}}} \end{aligned} \tag{B.11}$$

Equation (B.10) and Equation (B.11) are the expressions for SNR of WSK-WDM system considering Gaussian distribution for uniform and nonuniform dispersion fibers respectively. From Equations (B.1) and (B.2), the error probability or bit error rate (BER) of WSK-WDM transmission system can be expressed as

$$P_e = Q(x) = \frac{1}{2} erfc\left(\frac{x}{\sqrt{2}}\right) \tag{B.12}$$

APPENDIX C

Derivation of Expressions for Power Penalty and Allowable Input power of WSK-WDM System

The expression for SNR derived in Equation (B.10) will be used for the derivation of expressions for power penalty and allowable input power. Assuming $\sigma_F^{(m)^2} \approx \sigma_F^{(s)^2}$, the equation is again written here,

$$x = \frac{RP_r}{\sqrt{N_{FWM} + N_{th} + N_{sh}}}$$

The above equation can be written as

$$x = \frac{RP_r}{\sqrt{2R^2 P_r^2 \frac{P^3}{P_r} C_{im}^{mp} + N_{th} + k_s RP_r}}$$

$$2R^2 P_r^2 \frac{P^3}{P_r} C_{im}^{mp} + N_{th} + k_s RP_r = \frac{R^2 P_r^2}{x^2}$$

$$\frac{R^2}{x^2} P_r^2 - 2R^2 P_r^2 \frac{P^2}{P_r^p} C_{im}^{mp} - k_s RP_r - N_{th} = 0$$

$$aP_r^2 - bP_r - c = 0$$

$$P_r = \frac{b \pm \sqrt{b^2 + 4ac}}{2a} \tag{C.1}$$

This is the expression for received power considering FWM noise.

where $a = \frac{R^2}{x^2} - 2R^2 \frac{P^2}{P_r^p} C_{im}^{mp}$

$$b = k_s R$$

$$c = N_{th}$$

and $C_{im}^{mp} = \frac{P_r}{P^3} C_{im}^{m}$ with $C_{im}^{m} = \frac{1}{8}\sum_{I} P_{ijk} + \frac{1}{4}\sum_{II} P_{ijk}$

Here C_{im}^{m} is regarded as effective FWM crosstalk, P_{ijk} is the four-wave mixing power and P is the input power per channel. Next, the signal power to attain a given BER without influence of FWM is similarly derived with $C_{im}^{m} = 0$ as

$$P_{r0} = \frac{b \pm \sqrt{b^2 + 4a^p c}}{2a^p} \tag{C.2}$$

where $a^p = \frac{R^2}{x^2}$, b and c are as usual.

The power penalty of a communication system is defined as the ratio of received power considering FWM noise to the received power without the influence of FWM. Hence, The equation for the power penalty is obtained by dividing Equation (C.1) by Equation (C.2), and be written as

$$P_p = \frac{P_r}{P_{r0}} = \frac{(b + \sqrt{b^2 + 4ac})a^p}{(b + \sqrt{b^2 + 4a^p c})a} \tag{C.3}$$

This is the expression for the power penalty to achieve a given BER for WSK-WDM system. The Equation (C.3) is utilized to derive the expression for allowable input power per channel to attain a given BER. This equation can be written as

$$P_p \frac{a}{a^p} = \frac{b + \sqrt{b^2 + 4ac}}{b + \sqrt{b^2 + 4a^p c}}$$

$$b+\sqrt{b^2+4ac}=\left(b+\sqrt{b^2+4a^pc}\right)\left(P_p\frac{a}{a^p}\right)$$

$$4ac=\left(\left(b+\sqrt{b^2+4a^pc}\right)\left(P_p\frac{a}{a^p}\right)-b\right)^2-b^2$$

$$a=\frac{\left(\left(b+\sqrt{b^2+4a^pc}\right)\left(P_p\frac{a}{a^p}\right)-b\right)^2-b^2}{4c}$$

$$a^p-2R^2P^2\frac{C_{im}^{mp}}{P_r^p}=\frac{\left(\left(b+\sqrt{b^2+4a^pc}\right)\left(P_p\frac{a}{a^p}\right)-b\right)^2-b^2}{4c}$$

$$P=\left[\frac{P_r^p}{2R^2C_{im}^{mp}}\left\{a^p-\frac{\left(\left(b+\sqrt{b^2+4a^pc}\right)\left(P_p\frac{a}{a^p}\right)-b\right)^2-b^2}{4c}\right\}\right]^{1/2} \qquad \text{(C.4)}$$

where $P_r^p=\frac{P_r}{P}=L_re^{-\alpha L}$

This is the expression for allowable input power per channel of WSK-WDM transmission system in Gaussian approximation.